Study on the Developmental Stage-specific Cell Surface Protein of African Trypanosomes

（アフリカトリパノソーマ発育段階特異的細胞表面タンパク質に関する研究）

2016

The United Graduate School of Veterinary Sciences, Gifu University
(Obihiro University of Agriculture and Veterinary Medicine)

YAMASAKI, Shino

Study on the Developmental Stage-specific Cell Surface Protein of African Trypanosomes

（アフリカトリパノソーマ発育段階特異的細胞表面タンパク質に関する研究）

YAMASAKI, Shino

1. CONTENTS

2. ABBREVIATIONS

A	AA	Amino acid
	AAT	Animal African trypanosomosis
	α-rTcEpHbR	Anti recombinant *Trypanosoma congolense* epimastigote-specific free-hemoglobin receptor
	α-rTcHpHbR	Anti recombinant *T. congolense* haptoglobin-hemoglobin complex receptor
	ABC	ATP binding cassette
	ALA	Aminolevulinic acid
	ATP	Adenosine triphosphate
B	BSA	Bovine serum albumin
	BSF	Blood stream form
C	CESP	*Congolense* epimastigote specific protein
	CNS	Central nervous system
	CP-III	Coproporphyrinogen III
	CSF	Cerebrospinal fluid
D	DAB	3, 3'-diaminobenzidine
E	EDTA	Ethylenediaminetetraacetic acid
	ELISA	Enzyme-linked immunosorbent assay
	EMEM	Eagle's minimal essential medium
	EMF	Epimastigote form

F	FBS	Fetal bovine serum
	FITC	Fluorescein isothiocyanate
G	gDNA	Genomic DNA
	GST	Glutathione S-transferase
	GST-rTcEpHbR	GST-tagged recombinant *T. congolense* epimastigote-specific free-hemoglobin receptor
	GST-rTcHpHbR	GST-tagged recombinant *T. congolense* haptoglobin-hemoglobin complex receptor
H	HAT	Human African trypanosomosis
	Hb	Hemoglobin
	His	Six residues of histidine
	His-rTbHpHbR	His-tagged recombinant *T. brucei* haptoglobin-hemoglobin complex receptor
	His-rTcEpHbR	His-tagged recombinant *T. congolense* epimastigote-specific free-hemoglobin receptor
	His-rTcHpHbR	His-tagged recombinant *T. congolense* haptoglobin-hemoglobin complex receptor
	HMB	Hydroxymethyl bilane
	Hp	Haptoglobin
	HpHb	Haptoglobin-hemoglobin complex
	HEPES	4-(2-hydroxyethyl)-1-piperazineethanesulfonicacid
	HI-FBS	Heat inactivated FBS

	HMI-9	Hirumi’s modified Iscove’s medium-9
	HRP	Horseradish peroxidase
I	IFA	Indirect immunofluorescence assay
	Ig	Immunoglobulin
	i. v.	Intravenous injection
	IMDM	Iscove’s modified Dulbecco’s medium
K	K_d	Dissociation constants
L	LAMP	Loop-mediated isothermal amplification
M	mAb	Monoclonal antibody
	MOPS	3-N-morpholino propanesulfonic acid
P	PBG	Porphobilinogen
	PBS	Phosphate-buffered saline
	PBS-T	PBS containing 0.05% Tween 20
	PCF	Procyclic form
	PCR	Polymerase chain reaction
	PPG-IX	Protoporphyrinogen IX
	PP-IX	Protoporphyrin IX
	PSG	PBS containing 1% glucose
	PVDF	Polyvinylidene difluoride
R	RBC	Red blood cell
	rRNA	Ribosomal RNA
	rTcEpHbR	Recombinant TcEpHbR

	rTcHpHbR	Recombinant TcHpHbR
S	SAS	Saturated ammonium sulfate
	SDS	Sodium dodecyl sulfate
	SDS-PAGE	SDS-polyacrylamide gel electrophoresis
	SPR	Surface plasmon resonance
T	TBV	Transmission blocking vaccine
	TbHpHbR	*T. brucei* HpHb receptor
	tbhphbr	TbHpHbR gene
	TcEpHbR	*T. congolense* epimastigote-specific free-Hb receptor
	TcHpHbR	*T. congolense* HpHb receptor
	tchphbr	TcHpHbR gene
	TvHpHbR	*T. vivax* HpHb receptor
	TVM-1	*T. vivax* medium-1
U	UP-III	Uroporphyrinogen III
V	VSG	Variant surface glycoprotein

3. UNIT ABBREVIATIONS

B	bp	Base pair
D	ºC	Degree Celsius
H	h	Hour
K	kb	Kilobase
	kbp	Kilobase pair
	kDa	Kilodalton
L	L	Liter
M	µg	Microgram
	µL	Microliter
	µM	Micromolar
	mg	Milligram
	mL	Milliliter
	min	Minute
N	ng	Nanogram
R	RU	Resonance unit
U	U	Unit
V	V	Volt

4. GENERAL INTRODUCTION

I. African trypanosomosis

Threat of the disease

African trypanosomosis is one of the most important, arthropod-borne protozoan diseases which spread widely in sub-Saharan Africa. Human African trypanosomosis (HAT) is caused by *Trypanosoma brucei rhodesiense* and *T. b. gambiense,* and known as African sleeping sickness, which is lethal if left untreated (70). HAT threatens 65 millions of people and causes up to 20,000 new infections per year (136). Meanwhile, animal African trypanosomosis (AAT) is caused by *T. congolense, T. b. brucei* and *T. vivax,* and known as Nagana. The AAT prevents production of meat and milk, and causes an extensive economic loss, US$ 4.75 billion per year (73). Both the HAT and AAT are transmitted by tsetse fly (*Glossina* spp.) (3). This vehicle for spread of the diseases habitats in 37 countries in sub-Saharan Africa (Fig. 1) (3, 136, 140). They are quite serious constraints to both human life and livestock production in this area.

Clinical symptoms

In the clinical course, HAT is divided into two stages (136). In the hemolymphatic stage (stage 1), after the tsetse bite for blood meal, trypanosome parasites migrate to the draining lymph node and reach blood circulation. The parasites rapidly divide in the peripheral hemolymphatic systems. Subsequently, in meningoencephalitic stage (stage 2), *T. brucei* migrates to central nervous system

(CNS). Briefly, after the parasites proliferate in host blood stream, they invade CNS via the paracellular position of blood cerebrospinal border in accordance with population peaks in blood. Therefore, parasites travel along subarachnoid in the cerebrospinal fluid (CSF) and manifest between pial cells to evade from the trypanocidal effect of cerebrospinal fluid (86, 90, 108, 142). Finally, *T. brucei* infects to the brain parenchyma as the terminal stage of HAT (86, 90, 100, 101, 108, 129, 132, 142). *Trypanosoma brucei gambiense* infection follows chronic course over several months or years without any specific symptoms in the stage 1 (69). After invasion to CNS (stage 2), the disease progresses with immunosuppression, severe headache, sleep disorder, weight loss and endocrine abnormalities (70, 142). Neuropsychiatric symptoms also appear with painful paresthesis, disturbed rhythms and psychotic symptoms (100, 101, 142). Finally, a general wasting appears, and once brain invasion commences, the patient slips into a coma, followed by death (136). On the other hand, the infection with *T. b. rhodesiense* follows more acute course, and manifest higher fever, rapid coma and death within weeks (136).

The general clinical signs of AAT are parasitemia, intermittent fever, severe anemia, weight loss, reduced productivity caused by progressive weakness, abortion and infertility on breeding animals, and mortality during acute cases of diseases (83). Survivor becomes chronically infected for months or years, displaying low levels of fluctuating parasitemia, and serves as a reservoir for the diseases (93).

Diagnoses

The rapid and accurate diagnosis of African trypanosomosis is important for reducing the risk of disease progression, choice of medicine and prevention of the disease. Microscopic examination technique for direct detection of trypanosomes in blood and/or CSF is a classical, but reliable diagnosis method (110). Although this method is inexpensive and field-applicable, it has a low-sensitivity and is not suitable for mass screening (60). Serological techniques, such as card agglutination test (CATT), enzyme-linked immunosorbent assay (ELISA) and indirect fluorescence antibody assay (IFA), have been utilized for diagnosis and epidemiological surveillance of the trypanosomosis (28, 82, 98, 106). Although these serological methods are suitable for mass screening, they can not distinguish between the past and current infections. Recently, polymerase chain reaction (PCR)-based methods have been applied to the detection of trypanosome (15, 60). The advantages of this method are high-specificity, sensitivity, and rapid identification of the trypanosome species (40). In addition to the PCR methods, a loop-mediated isothermal amplification (LAMP) technique has been developed for the detection of African trypanosomes, as it is a more specific, sensitive, cost effective and field applicable diagnosis method than PCR ones (96, 97, 130, 131).

Treatments

All people diagnosed as HAT should have treatment. The specific drug and treatment course are depend on the trypanosome species (*T. b. gambiense* or *T. b. rhodesiense*) and the clinical stage (stage 1 or 2) (8). In the case of HAT, suramine and

pentamidine are commonly used for the hemolymphatic stage (stage 1). Suramine is used as the first choice for *T. b. rhodesiense,* while pentamidine is used for *T. b. gambiense* (8). In case of CNS stage (stage 2), melarsoprol is used as the traditional drug for both *T. b. rhodesiense* and *T. b. gambiense* infections (79, 136). An ornithine decarboxylase inhibitor, eflonithine, has been applied to the CNS stage of *T. b. gambiense* infection, especially for melarsoprol-refractory of trypanosomosis in 1981 (16, 79). Hereby, the first choice of treatment for *T. b. gambiense* is eflonithine, instead of melarsoprol (121). Furthermore, nifurtimox/eflonithine-combination treatment has been undergoing since 2003 (19). In the case of AAT, quinapyramine dimethosulfate, pyrothidium bromide, isometadium chloride, diminazene aceturate and suramine are generally used (126). In the endemic areas, quinapyramine dimethosulfate, pyrithidium bromide and isometamidium chloride are also used for the chemoprophylaxis (78).

Trypanocidal drugs listed above have significant problems. The main problem is severe side effects. For example, melarsoprol, a derivative of organic arsenical, causes a reactive encephalopathy in about a fifth of all patients receiving this treatment, while substantial proportion of the patients (2-12%) die (102, 135). Furthermore, unaffordable price (102), drug resistant parasites (4, 21), poor availability (79), drug residues (91) and emerging treatment failure (79) have been reported. However, the development of more effective trypanocidal drugs has not been vigorously pursued, as it is evidently not profitable for pharmaceutical companies (135).

II. Biology of African trypanosomes

Parasites and vectors

African trypanosomes belong to the genus *Trypanosoma* that is within phylum Euglenozoa, class Kinetoplastidae and order Trypanosomatida (87). HAT is caused by *T. b. gambiense* in West and Central Africa and by *T. b. rhodesiense* in East Africa (121, 136). On the other hand, AAT is caused by *T. b. brucei*, *T. vivax*, *T. congolense*, *T. simiae* and *T. godfreyi* (6, 89). All of these trypanosomes are biologically transmitted by tsetse flies (*Glossina*). *Glossina* consists of 31 species with three groups, namely *fusca*, *palpalis* and *morsitans,* and distributes from the south of Sahara and Somali deserts to north of Kalahari and Namib deserts in Africa (139). *Trypanosoma brucei gambiense* is transmitted by *G. palparis,* while *T. b. rhodesiense* is transmitted by *G. morsitans* (52). Because of this vector difference, the epidemic area of *T. b. gambiense* is the West and Central Africa, while that of *T. b. rhodesiense* is East Africa (52). On the other hand, *T. congolense* can be transmitted by several *Glossina* sp (43). Therefore, AAT spreads all over the tsetse distribution (http://www.fao.org/docrep/006/x0413e/x0413e02.htm#ref1.4.2). Because the tsetse distributions in Africa looks like a belt-shape, it is called “Tsetse belt” (140). .

Life cycle

African trypanosomes undergo cell differentiation events during their life cycle in tsetse and vertebrate host. The developmental stages of African trypanosome are divided into four stages, namely blood stream form (BSF), procyclic form (PCF),

epimastigote form (EMF) and metacyclic form (MCF) (20, 127). The BSF parasitizes interstitial space, blood, lymphatic or tissue fluid of vertebrate host. Although BSF parasites are generally natant, *T. congolense* BSF parasites have a remarkable affinity for endothelial cell layers and primarily accumulate at the walls of blood capillaries (117). The BSF stage of *T. brucei* is pleomorphic and divided into the replicating long slender and non-proliferative short stumpy forms (116). Only the stumpy form can adapt to tsetse midgut, and differentiate into PCF (47, 69, 83, 129). After the BSF parasites are ingested by tsetse fly, they immediately differentiate into the PCF in the midgut. The PCF parasites can proliferate in the tsetse midgut, and express PCF-stage specific surface proteins to protect the parasite against proteases of tsetse midgut (1, 5, 13, 42, 48, 111). The PCF differentiates into EMF, and migrates to labrum of tsetse proboscis (*T. congolense*) or salivary glands via proboscis (*T. brucei*) (99, 109). *Trypanosoma congolense* EMF strongly adheres to the lining of tsetse labrum or plastic surface of *in vitro* culture flask, using their flagella by their hemidesmosome-like structure (Fig. 2) (78, 123). In contrast, *T. brucei* EMF adheres to epithelium of tsetse salivary gland (Fig. 3) (9, 26, 80, 129). Finally, the EMF differentiates into non-adherent, non-proliferative but mammal-infective MCF that appears in tsetse hypopharynx (26). During bloodmeal, MCF parasites are inoculated into mammalian host, and they differentiates into BSF within 6 hs and then multiplies for a few days at the site of tsetse bite before invading the blood stream and lymphatics (112).

Trypanosoma congolense is the only African trypanosome that can be maintained stably *in vitro* (61). The BSF of *T. congolense* adheres weakly on the culture bottom by

using their flagellar while proliferate, and non-adherent BSF is contained in the supernatant (61). On the other hand, PCF is non-adherent and proliferates in the culture supernatant. After PCF is maintained for several weeks, The PCF differentiates into EMF. The EMF adheres strongly on the culture bottom and proliferates. MCF differentiates from the EMF, and floats in the EMF-culture supernatant. The main population is non-adherent EMF, and while minor population is MCF in the EMF-culture supernatant.

Immune evasion and vaccine

Vaccine is a quite useful tool for disease control. However, all attempts to establish effective vaccines against BSF have been unsuccessful, because BSF can evade host immune responses by antigenic variations of their dense variant surface glycoprotein (VSG) (56). Mammalian hosts infected with trypanosome raise the specific antibody to VSG coated on the surface of BSF cell, and the BSF parasites are eliminated from host bloodstream. However, since the antigenic variation of VSG continuously occurs within the population of infected trypanosome, the parasites can escape from recognition by the antibodies, in which the escape causes a prolonged infection (56). In addition, BSF can rapidly sweep out the antibodies which bind their VSG, by their endocytosis (95). Because of these mechanisms of antigenic variation of VSG and rapid antibody clearance, development of effective vaccine targeting BSF has not been achieved for a realistic field setting (74).

For controlling African trypanosomosis, transmission-blocking vaccine (TBV) is expected as a new prevention tool. The aim of TBV is to block and/or interfere with the parasite development in vector, and to repress the transmission to other mammalian hosts (31). TBVs target the proteins, which have essential/important function for survival of the parasites in vector or for vector itself (31). However, TBV for trypanosomosis has not been developed yet, although several TBV-candidate proteins have been reported for leishmaniosis, malaria and several tick borne diseases (32, 34, 39, 94, 107, 143).

III. The importance of heme for trypanosomes

Heme synthesis in eukaryotes

Many living organisms consume oxygen for energy production. Heme proteins, the proteins containing heme as co-factor, are greatly involved in the metabolism of oxygen. Heme proteins have essential roles in various biological activities. For example, cytochrome c, which is known as one of many heme proteins, is an essential component of electron transport chain (141). Catalase and peroxidase are also heme proteins, and they reduce levels of hydrogen peroxide and lipid peroxides to protect the organism from oxidative damage (16). Cytochrome P450 is the superfamily protein containing heme. The P450 can catalyze a variety of molecules as substrates, and involve the drug metabolism (56, 84, 141). In addition, because of high oxidative activity of heme, organisms have heme homeostasis mechanism to avoid not only heme deficiency but also the excess (71). Thus, heme is an essential molecular for living organisms, because the heme proteins contribute to many biological functions.

Because of such a high biological necessity of heme, eukaryotes are generally capable of *de novo* heme synthesis (10). Shown in Fig. 4, heme is synthesized from succinyl Co-A and glycine through eight catalytic steps, and then incorporated into heme proteins, such as cytochrome *c* and peroxidase (9, 80). In eukaryotes, 5-aminolevulinic acids (ALA) synthesis from succinyl Co-A and glycine by ALA-synthase in mitochondrion is the first step of heme synthesis (100, 118). After transportation of ALA from mitochondrion to cytoplasm, two molecules of ALA are combined, and become a porphobilinogen (PBG) by ALA-dehydrogenase (11). Four

molecules of PBG are combined through a deamination into a hydroxymethyl bilane (HMB) by PBG-deaminase (114). Then, HMB is hydrolysed to form a circular tetrapyrrole uroporphyrinogen III (UP-III) by UP-III synthase (53), and the UP-III is decarboxylated into a coproporphyrinogen III (CP-III) by UP-III decarboxylase (64, 126). Protoporphyrinogen IX (PPG-IX), which is a CP-III oxide by CP-III oxidase, is transported to mitochondrion (62). The PPG-IX is further oxidized by PPG-IX oxidase, and become a protoporphyrin IX (PP-IX) (12). The PP-IX is a precursor of many metalloporphyrins, including heme (58, 81). Heme, which is combined with iron ion by ferrochelatase, is one of metalloporphyrins (101). The heme, synthesized via this system, consists into many proteins and plays many important roles as co-factor of heme proteins.

Hemoglobin metabolism

Hemoglobin (Hb), a tetramer protein containing heme, is contained in red blood cell (RBC) and transports oxygen to whole body (29). Fetal Hb can bind to the oxygen with a greater affinity than adult Hb to get enough oxygen from maternal (36). Unlike adult Hb consisting α-subunit and β-subunit, fetal Hb consists of the α-subunit and γ-subunit (7, 104, 115).

Because Hb has a high oxidative reactivity, the released Hb from RBC by hemolysis can injure other cells, oxidatively (41). Haptoglobin (Hp), one of serum proteins, immediately binds to the released Hb and constitutes a haptoglobin-hemoglobin complex (HpHb) to protect the tissue and cells from oxidative

damage (21, 105). After constitution of the HpHb, HpHb is scavenged by macrophage via CD163 receptor and digested in the lysosome of macrophage (105, 132). Finally, the heme is released from digested Hb and degenerated into innocuous bilirubin (132).

Heme uptake in Trypanosomatida

As described above, heme is an essential molecule for almost all living organisms as a component of many heme proteins, in which almost all eukaryotes have a *de novo* heme synthesis pathway highly conserved among organisms (9, 27, 37, 141). On the other hand, previous studies and a whole genome analysis revealed that trypanosomatids, such as *Trypanosoma* and *Leishmania*, lacked key enzymes for the heme biosynthesis (14, 26, 113). *Trypanosoma* parasites lack all of the heme synthases (ALA-synthase, ALA-dehydrogenase, PBG-deaminase, UP-III synthase, UP-III decarboxylase, CP-III oxidase, PPG-IX oxidase and ferrochelatase, shown in the blue and red boxes of Fig. 4) while *Leishmania* parasites lack ALA-synthase and ALA-dehydrogenase (Fig. 4, red boxes (26)). These parasites, therefore, are considered to depend on their hosts as a source of heme (134). Hb- and heme-uptake mechanisms have ever been studied in *T. cruzi*, *T. brucei* and *Leishmania* spp. The *T. cruzi* possesses an ATP-binding cassette (ABC) transporter for Hb uptake, whereas *Leishmania* spp. have an Hb receptor and an ABC transporter (24, 33, 63, 77). On the other hand, *T. brucei* possesses a haptoglobin (Hp)-Hb complex receptor (TbHpHbR), which is exclusively expressed in the BSF of parasite (138). After Hb (or HpHb)-binding to the uptake receptors, the Hb are endocytosed, mediated by clathrin, and transported to

lysosome via early/late endosome (23). The Hb are digested in the lysosome, and heme are released, from the digested Hb. Heme are transported to cytosol via heme transporters that are present at the lysosome membrane, and then utilized to produce various heme proteins (23). The heme proteins play the various and important roles for the surviving of trypanosome, such as mitochondrial respiration, antioxidant activity and so on (133).

IV. Objective of this study

Development of new control methods for HAT and AAT has been strongly desired for a long period, because of difficulty of the development of effective vaccine and trypanocidal medicine. The objective of this study was set to clarify heme-uptake mechanism in African trypanosome, in order to develop a new control strategy for HAT and AAT. *Trypanosoma congolense*, the most pathogenic parasite of Nagana, was chosen as my research material, because *T. congolense* is the only African trypanosome that all stages of their life cycle can be continuously maintained *in vitro* (61). In chapter I, I identified a *T. congolense* epimastigote-specific free-hemoglobin receptor (TcEpHbR). In chapter II, I evaluated the potential of TcEpHbR as a candidate molecule for TBV against African trypanosomosis.

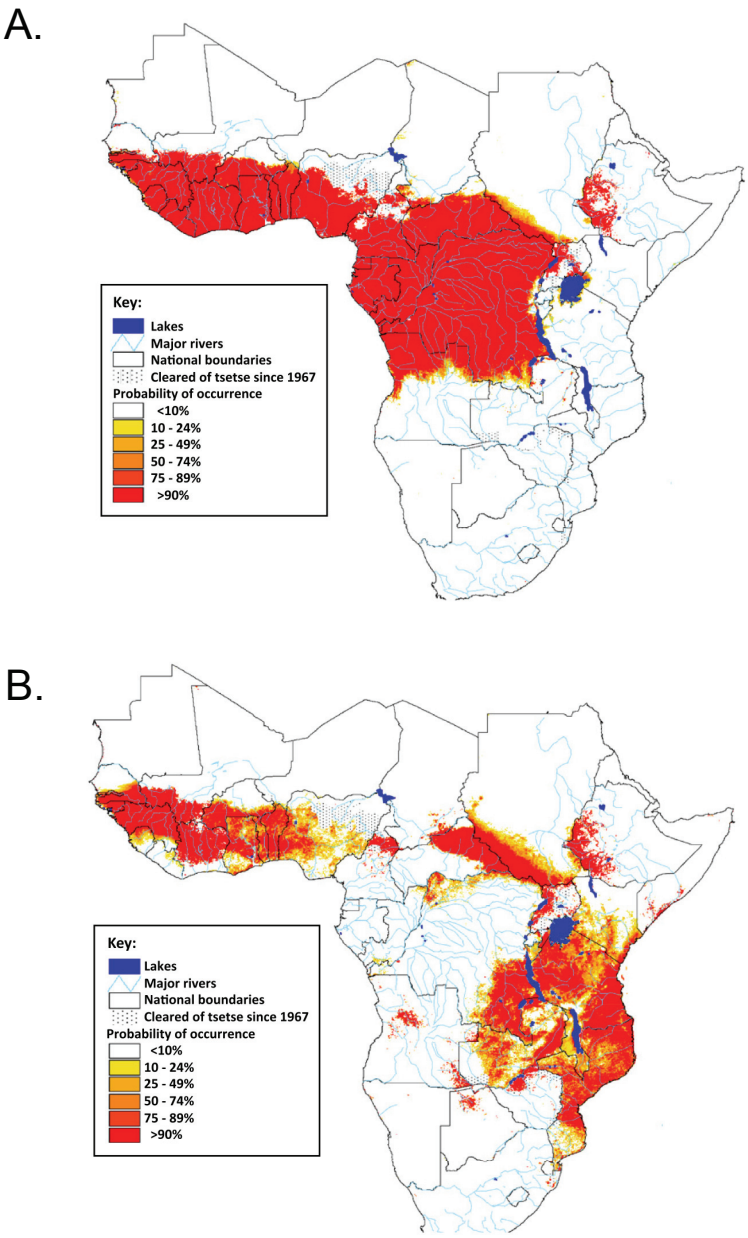

Fig. 1. Predicted distribution of tsetse fly. The underlying data were modified by the information from a wide range of sources, and incorporated into these analyses, including eco-climatic data, elevation cattle density, cultivation level, and human population for the prediction of the tsetse-flies distribution (http://www.fao.org/ag/againfo/programmes/en/paat/documents/maps/pdf/ tserep.pdf.). **A:** The potential range of *Glossina palpalis* group tsetse flies transmitting *T. b. gambiense*. **B:** The potential range of *G. morsitans* group tsetse flies transmitting *T. b. rhodesiense* (140).

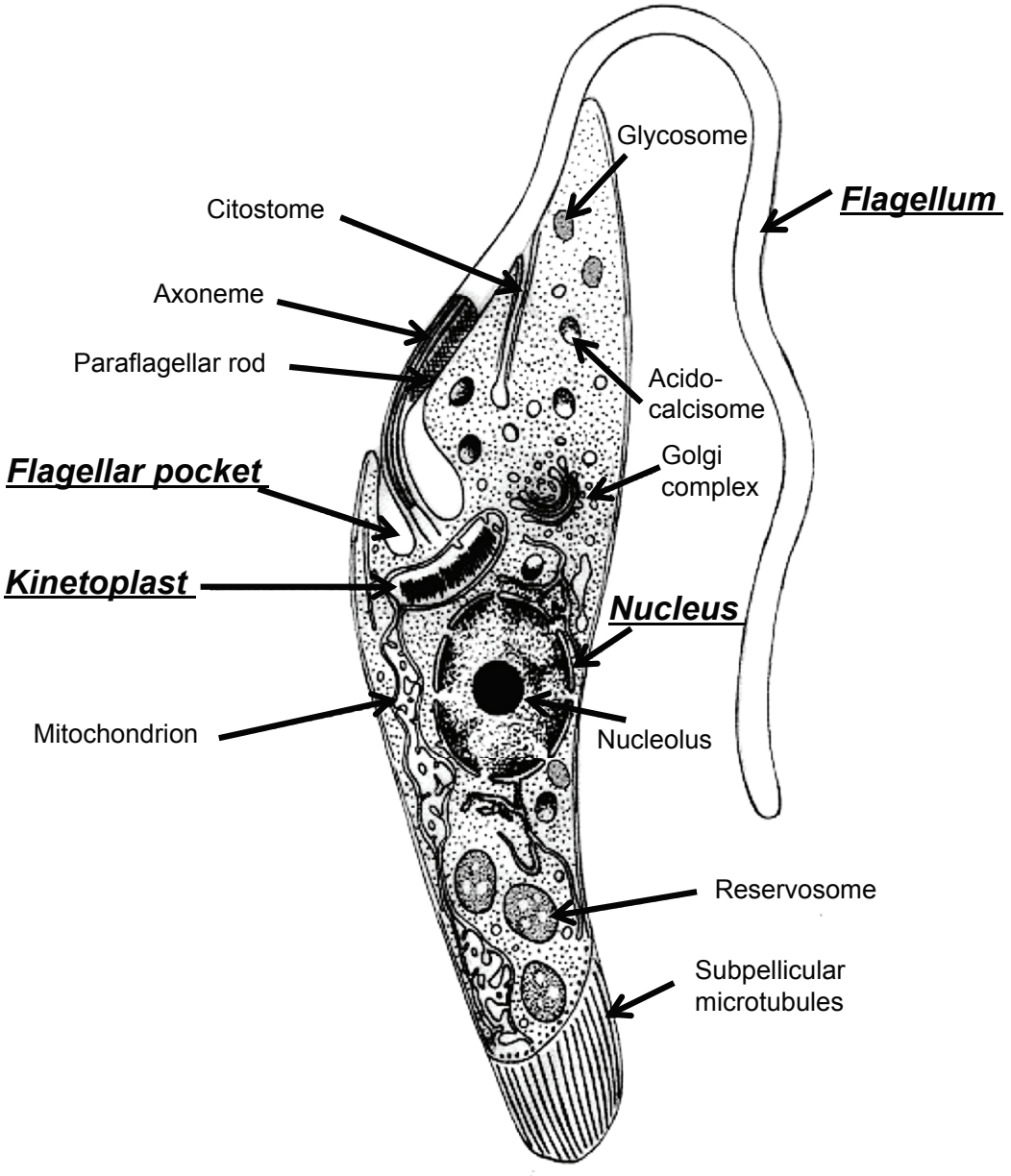

Fig. 2. Morphological schema of *Trypanosoma* EMF parasite. The EMF parasites can attach the proboscis or salivary gland by using their flagella (45, 129). The kinetoplast in EMF is located at the anterior vicinity of the nucleus in the cell (99). The endo/exocytosis in trypanosomes are performed by the flagellar pocket that is the flagellar invagination into the cell body (50). This figure was cited from Souza, 1999 and edited (123).

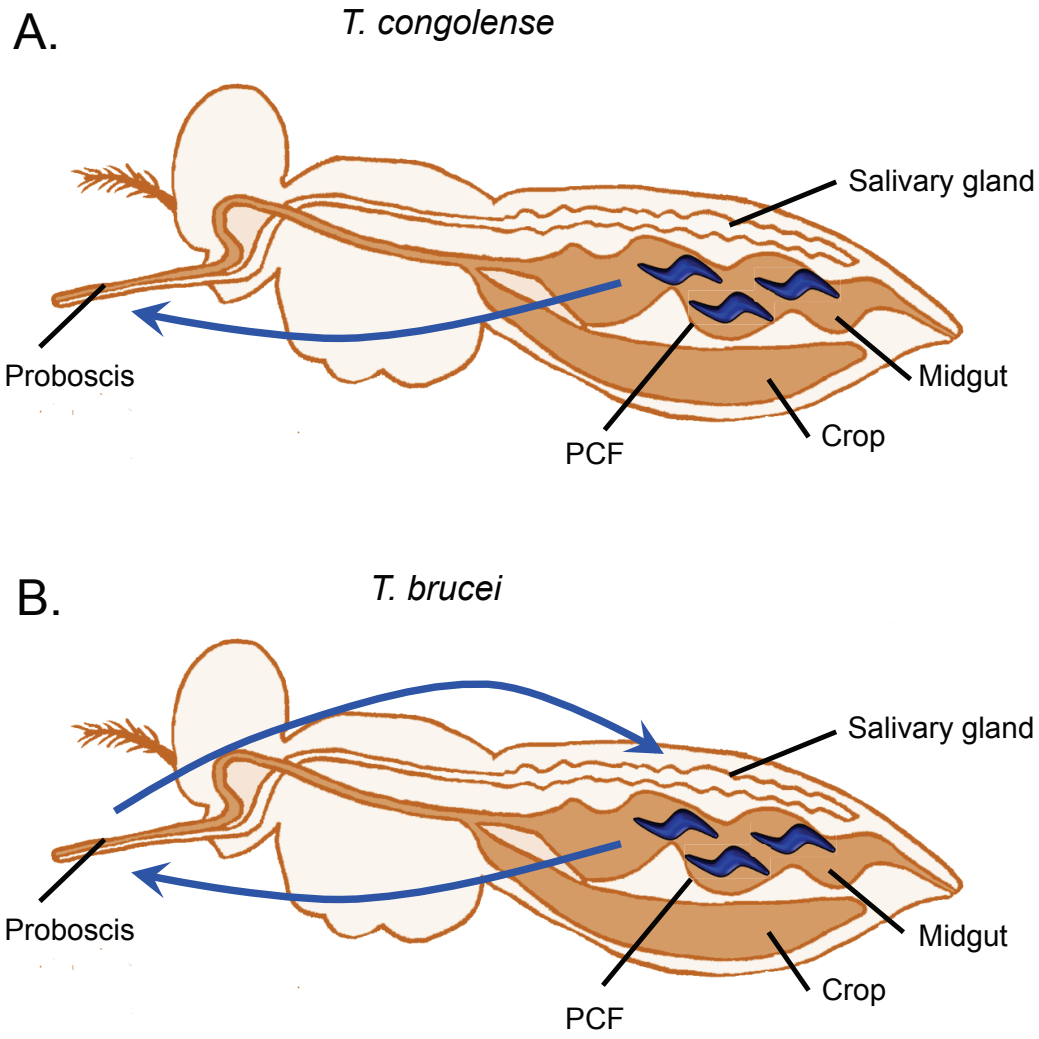

Fig. 3. Comparison of the PCF and EMF parasitisms of *T. congolense* and *T. brucei* in tsetse fly. A: After *T. congolense* PCF proliferates in tsetse midgut, it differentiates into EMF and migrates into proboscis. *Trypanosoma congolene* EMF strongly adheres to the lining of tsetse proboscis using its flagella. **B:** After *T. brucei* PCF proliferates in tsetse midgut, it differentiates into EMF and migrates into salivary gland of tsetse fly via proboscis. Finally, *T. brucei* EMF adheres to the epithelium of salivary gland of tsetse fly.

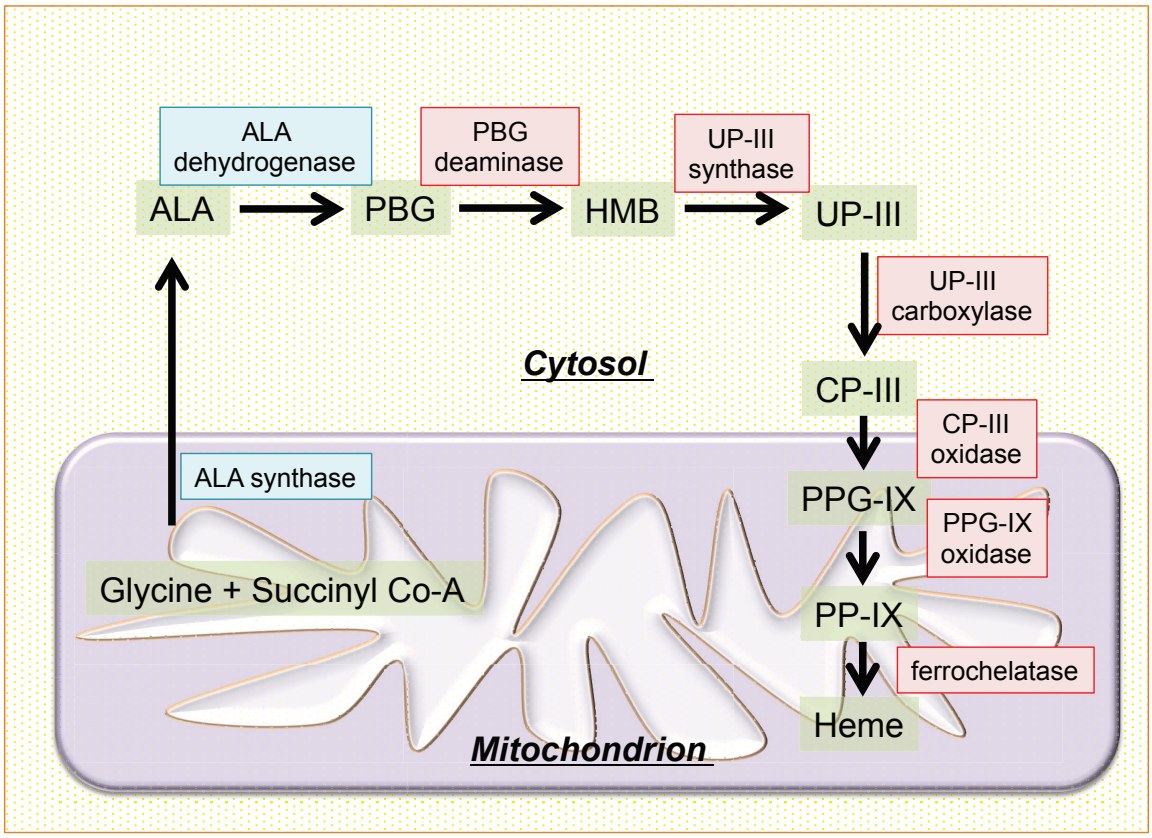

Fig. 4. Heme-synthesis pathway in eukaryote cell. Heme is synthesized from glycine and succinyl Co-A via 8 catalytic reactions. *Trypanosoma* lacks the enzymes in both of blue and red boxes, while *Leishmania* has the enzymes indicated in red boxes.

5. CHAPTER I

Characterization of an epimastigote-stage-specific hemoglobin receptor of *Trypanosoma congolense*

5-1. Introduction

In this chapter, I aimed to identify the hemoglobin (Hb)-uptake receptor and analyze the Hb uptake in all life cycle stages of *Trypanosoma congolense in vitro.* Previously, a haptoglobin (Hp)-Hb complex receptor (HpHbR) had been identified in *T. brucei,* and named as *T. brucei* HpHbR (TbHpHbR, Gene ID: Tb927.6.440), which is exclusively expressed in the blood stream form (BSF) of the parasite (138). In mammalian blood, Hb, which was released through a hemolysis, immediately binds to Hp to form a complex (HpHb), which is immediately detoxified and taken up by macrophages for Hb metabolism (72). In mammalian blood stream, *T. brucei* BSF also take up the Hb as HpHb via TbHpHbR (59, 138). Firstly, HpHb, when bound to TbHpHbR, is taken up into the BSF of *T. brucei* by clathrin-mediated endocytosis via flagellar pocket (88). Next, the endosomes including HpHb are transported to lysosome, and the cargo proteins are digested there (23). Heme contained in Hb is then released within lysosome, and transported to cytosol by *T. brucei* heme response gene protein, to be used for heme proteins (23). On the other hand, it had been only predicted that *T. congolense* also possessed an orthologue of the *tbhphbr, T. congolense* HpHbR (TcHpHbR, Gene ID: TcIL3000.10.2930) (46). Interestingly, an exhaustive proteome

analysis suggested that, unlike TbHpHbR, the TcHpHbR might be exclusively expressed in the epimastigote form (EMF) of *T. congolense* (46, 75). The vector stages of trypanosomes, particularly the procyclic form (PCF) and EMF, appear to require a greater amount of heme than the BSF, due to their fully activated cytochrome-mediated mitochondrial respirations (18, 85). However, the mechanisms underlying heme or Hb uptake still remain to be elucidated in the vector stages of African trypanosomes. The tsetse fly (*Glossina* spp.), which is the sole vector of African trypanosomes, periodically ingests blood meals from mammalian hosts, and free Hb is released from hemolyzed red blood cells (RBCs). Thus, it has been expected that the vector stages of the parasite would be exposed to a high concentration of free Hb derived from each blood meal of the tsetse fly. Based on the data of proteomic analysis (46), therefore, I also hypothesized that the TcHpHbR would be the EMF-specific Hb receptor of the parasite. As *T. congolense* IL3000 (TcIL3000) strain can be cultured in all of the four main life cycle stages *in vitro* (30, 61, 92), I utilized this cell line to characterize the developmental expression of TcHpHbR, and analyzed the Hb uptake in all of the life cycle stages.

5-2. Materials and Methods

Trypanosomes and culture conditions

TcIL3000 strain, which had been isolated near the border of Kenya and Tanzania in 1966 (according to the records of the Biological Service Unit at the International Livestock Research Institute, Nairobi, Kenya), and *T. b. brucei* GUTat 3.1 (Tbb GUTat 3.1) strain, which had been isolated in Uganda in 1966, were used in this study. The *T. congolense* and *T. brucei* BSF parasites were cultured in Hirumi's Modified Iscove's medium-9 (HMI-9) at 33ºC or 37ºC, respectively (17, 51, 60, 61). The HMI-9 composed of Iscove's Modified Dulbecco's Medium (IMDM, Sigma-Aldrich Co., MO, U. S. A.) supplemented with 100 U/L penicillin-100 μg/mL streptomycin (Thermo Fisher Scientific Inc., Waltham, MA, U. S. A.), 2 mM L-glutamine (Thermo Fisher Scientific Inc.), 0.1 mM bathocuproine (Sigma-Aldrich Co.), 1 mM sodium pyruvate (Sigma-Aldrich Co.), 10 μg/mL insulin, 5.5 μg/mL transferrin, 5.0 ng/mL sodium selenite (ITS-X supplement, Thermo Fisher Scientific Inc.), 1 mM sodium hypoxanthine, 16 μM thymidine (HT supplement, Thermo Fisher Scientific Inc.), 0.001% 2-mercaptoethanol (Sigma-Aldrich Co.), 2 mM L-cysteine (Sigma-Aldrich Co.), 0.4 g/L bovine serum albumin (BSA, Sigma-Aldrich Co.), 60 mM HEPES (Sigma-Aldrich Co.), and 20% fetal bovine serum (FBS, 178 μg/mL Hb, Batch No. S10123S1650, Biowest, Nuaillé, France) (61). The *T. congolense* PCF and EMF parasites were cultured in *T. vivax* medium-1 (TVM-1) at 27ºC (30). The TVM-1 composed of Eagle's Minimum Essential Medium (EMEM, Sigma-Aldrich Co.)

supplemented with 60 mM HEPES, 10 mM L-prorine (Sigma-Aldrich Co.) and 20% FBS (61). The *T. congolense* MCF was separated from the supernatant of culture, while the *T. congolense* EMF was confluently grown, was purified using anion-exchange column chromatography (DE 52, GE Healthcare Bio-Sciences Corp., Little Chalfont, U. K.) (76).

Nucleic acid extraction

Trypanosoma congolense and *T. b. brucei* BSF parasites were separated from each culture supernatant by centrifugation at 1,500 x *g* for 10 min at 4ºC. The parasite pellets were resuspended in a DNA extraction buffer (150 mM NaCl, 10 mM Tris-HCl (pH. 8.0), 10 mM EDTA and 0.1% sodium dodecyl sulfate (SDS)) containing 100 μg/mL Proteinase K (Wako Pure Chemicals Industries Ltd., Osaka, Japan), and incubated over night at 55ºC. The genomic DNAs (gDNAs) were purified from the suspension by twice extractions with phenol-chloroform-isoamylalcohol (Sigma-Aldrich Co.) and twice extractions with chloroform (Wako Pure Chemicals Industries Ltd.). Subsequently, the extracted gDNAs were precipitated by adding with 0.1 volume of 3 M sodium acetate (pH 5.5) and 1 volume of isopropyl alcohol (Wako Pure Chemicals Industries Ltd.). After centrifugation at 22,500 x *g* for 20 min at 4ºC, the pellet was rinsed with 75% ethanol (Wako Pure Chemicals Industries Ltd.), air-dried and dissolved in a distilled water. Extracted gDNAs were stored at -30ºC until use.

On the other hand, total RNAs of parasites were extracted from each stage of the

cultured TcIL3000 parasites. The BSF and PCF parasites were purified from each culture supernatant by centrifugation at 1,500 x *g* for 10 min at 4ºC, and then washed three times with phosphate-buffered saline (PBS). The flask of EMF culture was washed with PBS three times to remove the non-adherent cells. The MCF parasites were purified from EMF culture supernatant by DE 52 column chromatography. The float cells (BSF, PCF and MCF) were collected by centrifugation at 1,500 x *g* for 10 min at 4ºC, and then resuspended in a TRIzol reagent (Thermo Fisher Scientific Inc.). The TRIzol reagent was directly added into the washed EMF-cultured flask, and then collected by a cell scraper. The total RNAs were extracted following manufacture instructions of the TRIzol reagent, and dissolved in a DNase/RNase-free water (Thermo Fisher Scientific Inc.). Extracted total RNAs were stored at -80ºC until use.

Gene cloning and *in silico* amino acid (AA) sequence analysis

Fragments of the *tchphbr* and *tbhphbr* were amplified by PCR using a *Taq*-polymerase (Thermo Fisher Scientific Inc.) from gDNAs of TcIL3000 and TbbGUTat 3.1, respectively. The PCR primers were designed to remove the signal sequences and glycosylphosphatidylinositol-anchor-modified sequences because these regions were of high hydrophobicity (Table 1). The truncated *tchphbr* and *tbhphbr* fragments were TA-cloned into a pCR^{TM} 2.1 cloning vector (Thermo Fisher Scientific Inc.), and then transformed into Mach1 *Escherichia coli* (Thermo Fisher Scientific Inc.). The nucleotide sequence of *tchphbr* was determined using an automatedsequencer (3100 Genetic Analyzer, Thermo Fisher Scientific) with a BigDye Terminator Cycle

Sequencing kit (Thermo Fisher Scientific Inc.). The determined nucleic sequence of *tchphbr* was translated into AA sequence using a GENETIX software (GENETIX CORPORATION, Tokyo, Japan), and AA sequence alignments were performed among the deduced TcHpHbR, and obtained TcHpHbR candidate and TbHpHbR sequences from the kinetoplastid genomic resource (TriTrypDB, http://tritrypdb.org/tritrypdb/) by an alignment software (ClustalW, http://clustalw.ddbj.nig.ac.jp). The three-dimensional structure of TcHpHbR and TbHpHbR were predicted by using a structure-prediction software (I-TASSER, http://zhanglab.ccmb.med.umich.edu/I-TASSER/).

Production of recombinant TcHpHbR and TbHpHbR proteins

The truncated *tchphbr* and *tbhphbr* were subcloned into a pET28a (Novagen Merck Millipore, Darmstadt, Germany) or pGEX6p-1 (GE Healthcare Bio-Sciences Corp.) plasmids to produce his- or GST-tagged recombinant proteins, respectively. Prepared expression plasmids were transfected into BL21 *E. coli*. The expressions of his-tagged and GST-tagged recombinant proteins were induced in the BL21 by adding with 100 μM isopropyl-β -thiogalactoside (Wako Pure Chemicals Industries Ltd.) at 37ºC for 5 hs with a gentle agitation. After the induction, *E. coli* was collected by centrifugation at 13,000 x *g* for 10 min at 4ºC, and resuspended in PBS. Fifty micrograms per milliliter lysozyme were added to the suspension, and then incubated for over night at 4ºC with a gentle agitation. Next, the suspension was sonicated for 5 min on ice, and then centrifuged at 13,000 x *g* for 10 min at 4ºC. From the supernatant, the his-tagged or GST-tagged proteins were purified using an Ni-beads column

(QIAGEN, Venlo, Netherland) or a glutathione sepharose beads column (GE Healthcare Bio-Sciences Corp.), respectively. In detail, to immobilize the recombinant proteins bound on the affinity beads, the supernatant containing his-tagged or GST-tagged recombinant proteins were added into Ni-beads column or glutathione sepharose beads column, respectively, and the columns were incubated at 4ºC for over night with a gentle agitation. The recombinant proteins-immobilized beads were washed three times with PBS. Then, the his-tagged recombinant proteins immobilized on Ni-beads column were eluted by an elution buffer (100 mM $NaPO_4$, 10 mM Tris-HCl, 200 mM imidazole, pH 6.3). In contrast, GST-tagged recombinant proteins immobilized on glutathione sepharose beads column were eluted by a GST elution buffer (50 mM Tris-HCl (pH 8.0), 16 mM reduced glutathione), or cleaved the GST-tag from recombinant protein by a prescission protease buffer (50 mM Tris-HCl (pH. 7.0), 150 mM NaCl, 1 mM EDTA) containing 160 U/mL precision protease (GE Healthcare Bio-Sciences Corp.). The eluted recombinant proteins were dialyzed three times using a dialysis membrane (Thermo Fisher Scientific Inc.) against 1 L of PBS at 4ºC. Finally, concentrations of the recombinant proteins were measured using a protein colorimetric assay kit (Thermo Fisher Scientific Inc.), and then adjusted to the final concentration of 1 mg/mL prior to use. The GST-tagged recombinant proteins were used as the bait protein for GST pull-down assay, while his-tagged recombinant proteins were used for immunization. These recombinant proteins were kept at -30ºC until use.

Immunization

Five female 7-week-old Jcl:ICR mice (CLEA Japan, Inc., Tokyo, Japan) were immunized with 50 μg (50 μL in volume) of his-tagged recombinant TcHpHbR (his-rTcHpHbR), which was emulsified in an equal volume of adjuvant TITERMAX® GOLD (TiterMax U. S. A. Inc., Norcross, U. S. A.). The immunizations were performed by subcutaneous injection (one primary and four booster injections) at 2-week intervals. Two weeks after the last booster injection, blood was collected by cardiac puncture at terminal anesthesia. Serum was prepared by centrifugation of the coagulated blood at 15,000 x *g* for 1 min at room temperature (RT). The animal experiments were performed in accordance with the standards of animal experimentations in Obihiro University of Agriculture and Veterinary Medicine (approval No. 27-92).

Southern blot analysis

Ten micrograms of gDNAs extracted from TcIL3000 were digested with a restriction enzyme, *Nsi*I (Roche Diagnostics K. K., Tokyo, Japan), *Sac*II or *Pst*I (New England Bio Labs, MA, U. S. A.). After the digestion by restriction enzyme, the DNAs (10 μg/well) were separated in a 1% agarose gel. The electrophoretically separated DNAs were transferred onto a nylon membrane (GE Healthcare Bio-Sciences Corp.). The probe that was PCR-amplified using the TcHpHbR-SG primer pairs (Table 1), was labeled by using a DNA labeling kit (Alkphos Direct Labeling Reagent, GE Healthcare Bio-Sciences Corp.). The blotted membrane was hybridized with the alkaline

phosphatase-labeled DNA probe under a high stringency condition. For visualizing, the membrane was incubated in a CDP-STAR detection reagent (GE Healthcare Bio-Sciences Corp.), following the manufacture's instruction. The membrane was exposed onto an X-ray film (GE Healthcare Bio-Sciences Corp.), and the signals were detected using the developing machine (CEPROSQ, FUJIFILM, Tokyo, Japan)

Northern blot analysis

Ten micrograms of total RNAs were separated on a 0.8% agarose gel containing 2.2 M formaldehyde in a 3-N-morpholino propanesulfonic acid (MOPS) buffer. The RNAs were transferred onto a nylon membrane (GE Healthcare Bio-Sciences Corp.), and then, the membrane was then fixed by UV-induced crosslinking using a UV cross linker (UVC 500, Hoefer, CA, U. S. A.). The transferred RNAs were probed with the alkaline phosphatase-labeled DNA probe distributed above, under a high-stringency condition. The DNA probes used for Southern blot analyses were reused to detect the TcHpHbR mRNA. The DNA probes to detect the internal reference transcript (18S ribosomal RNA, rRNA) were prepared by PCR using the primers shown in Table 1 (128). The signals were detected, following the method described above.

Western blot analysis

Total proteins were extracted from each life stage of *T. congolense* by incubating in a cell lysis buffer (20 mM Tris-HCl pH 8.0, 150 mM NaCl, 1 mM $MgCl_2$, 1 mM $CaCl_2$, 10% glycerol, 1% Triton-X 100, protease inhibitor cocktail (Roche Diagnostics

K. K.)) for 4 hs at 4ºC. Concentrations of the total proteins were measured in the protein colorimetric assay described above. The extracted proteins (2 μg) were separated by 10% SDS-polyacrylamide gel electrophoresis (SDS-PAGE), and electrophoretically transferred onto a polyvinylidene difluoride (PVDF) membrane (GE Healthcare Bio-Sciences Corp.). After blocking of the membrane in 5% skim milk PBS at RT for 1h, the blotted membrane was incubated with the anti-rTcHpHbR (α-rTcHpHbR) mouse immune serum diluted at 1:1,000 with PBS as 1st antibody at 27ºC for 1 h. The membrane was washed three times with PBS containing 0.05% Tween 20 (PBS-T), and then incubated with anti-mouse IgG conjugated with horseradish peroxidase (HRP) (GE Healthcare Bio-Sciences Corp.) (1:2,500 in PBS) at 27ºC for 1 h. After washing with PBS-T for three times, the signals were detected in a 3, 3'-diaminobenzidine detection system (DAB, Sigma-Aldrich Co.).

Indirect fluorescent antibody method (IFA)

The BSF, PCF, and EMF of parasites were collected from culture supernatants. The MCF cells were purified from EMF culture supernatant by DE 52 column chromatography (76). Collected cells were washed three times with PBS. The cell suspensions were spread over glass slides (MATSUNAMI GLASS IND., LTD, Osaka, Japan), air-dried and fixed with 100% methanol. The specimens were incubated with α-rTcHpHbR mouse immune serum at 1:100 dilution and 20 μg/mL biotinylated tomato lectin (Vector Laboratories, Burlingame, U. S. A.) to label the endocytic compartments (flagellar pocket and endosome) (120). After washing with PBS-T, the slides were

incubated with 1:200 diluted anti-mouse IgG conjugated with fluorescein isothiocyanate (FITC, Thermo Fisher Scientific Inc.) and 30 μg/mL streptavidin conjugated with fluorochrome (Vector laboratories). Nucleus and kinetoplast DNAs were stained with Hoechst 33342 (Dojindo, Kumamoto, Japan). A confocal laser scanning microscope (Leica Microsystems GmbH, Wetzlar, Germany) was used to observe the prepared specimens.

The analyses of hemoglobin (Hb) and haptoglobin (Hp) uptakes to trypanosome

RBCs purified from defibrinated bovine whole blood (22) were washed three times in PBS by centrifugation at 910 x *g* for 7 min at 4ºC. The RBCs were then resuspended in PBS, diluted 10 times with sterilized distilled water to induce a hemolysis by the hypoosmotic stress (54, 124) and then centrifuged at 15,000 x *g* for 10 min at 4ºC. The supernatant was lyophilized by using a freeze-drier (VD-500R, TAITEC, Saitama, Japan), and the obtained bovine Hb powder was kept at -30ºC until use. Bovine Hb and commercially purchased bovine Hp (Life Diagnostics Inc., West Chester, U. S. A.) were labeled with Alexa 488 (Hb^{A488} and Hp^{A488}, respectively) (Thermo Fisher Scientific Inc.). Hp^{A488}Hb complex was prepared by mixing equal volumes of 2 mg/mL Hp^{A488} and 2 mg/mL Hb solutions for 30 min at 37ºC. The TcIL3000 PCF, EMF and MCF were incubated in TVM-1 medium with 20 μg/mL of the Hb^{A488}, Hp^{A488} or Hp^{A488}Hb complex for 2.5 hs at 27ºC, while TcIL3000 BSF parasites were incubated in HMI-9 medium with 20 μg/mL of the Hb^{A488}, Hp^{A488} or Hp^{A488}Hb complex for 2.5 hs at 33ºC (61). Thereafter, the parasites were washed three

times with PBS, placed on glass slides, air-dried and fixed with 100% methanol for 10 min at RT. Nucleus and kinetoplast DNAs were stained with Hoechst 33342 for 30 min at 37ºC. The fixed parasites were incubated with PBS containing 20 μg/mL biotinylated tomato lectin for 1 h at 37ºC. The parasites were then washed with PBS-T for three times, and then incubated with PBS containing 30 μg/mL fluorochrome-labeled streptavidin for 1 h at 37ºC. A confocal laser scanning microscope (TCS-NT, Leica Microsystems GmbH) was used to observe the prepared specimens.

GST pull-down assay

To qualitatively analyze the interaction between TcHpHbR and its ligand (bovine Hb), a GST pull-down assay was performed using GST-tagged recombinant TcHpHbR (GST-rTcHpHbR) with glutathione sepharose beads 4B. The GST-rTcHpHbR and beads were incubated with 2 mg/mL Hb in PBS, FBS diluted twice with PBS, or PBS with a gentle agitation at 4ºC for overnight. After washing with PBS, the immobilized proteins to glutathione sepharose beads 4B were eluted with an SDS sample buffer (125 mM Tris pH 6.8, 10% 2-mercaptomethanol, 4% sodium dodecyl sulfate, 10% sucrose, 0.01% bromophenol blue), and then incubated at 98ºC for 5 min. Finally, the eluted samples were separated by 15% SDS-PAGE, and stained with a Coomassie Brilliant Blue R-250 (CBB, Wako Pure Chemicals Industries Ltd.).

Surface plasmon resonance (SPR) assay

Detail interactions between TcHpHbR and its ligand (bovine Hb, Hp and HpHb)

were measured in an SPR assay. The SPR assay was performed using a Biacore X analytical system (GE healthcare Bio-Sciences Corp.). The qualitative interactions between the his-rTcHpHbR or his-tagged recombinant TbHpHbR (his-rTbHpHbR) and the analytes (free-Hb, free-Hp or HpHb complex) were measured at a flow rate of 20 μL/min. Free-Hb and free-Hp were diluted to 1 μg/mL, 10 μg/mL and 100 μg/mL with a running buffer (HBS-EP, GE Healthcare Bio-Sciences Corp.). Hp-Hb complexes were prepared by the conjugating free-Hp and free-Hb at various concentrations; HpHb 10-50 (Hp 10 μg/mL and Hb 50 μg/mL), HpHb 50-50 (Hp 50 μg/mL and Hb 50 μg/mL), HpHb 100-50 (Hp 100 μg/mL and Hb 50 μg/mL), HpHb 50-10 (Hp 50 μg/mL and Hb 10 μg/mL) and HpHb 50-100 (Hp 50 μg/mL and Hb 100 μg/mL). His-rTcHpHbR and his-rTbHpHbR were diluted to 100 μg/mL with 10 mM sodium acetate, pH 4.5 (GE Healthcare Bio-Sciences Corp.) and coupled on the surface of CM5 sensor chips (GE healthcare Bio-Sciences Corp.). The final amounts of immobilized his-rTcHpHbR and his-rTbHpHbR were 5,450 resonance unit (RU) and 8,000 RU, respectively.

The quantitative interactions between recombinant proteins and analytes were measured at a flow rate of 20 μL/min. Free-Hb and free-Hp were serially diluted to 10, 1, 0.1, 0.01, 0.001, and 0.0001 μM with HBS-ER as analyte solutions. His-rTcHpHbR and his-rTbHpHbR were diluted to 10 μg/mL with 10 mM sodium acetate (pH 4.5), and immobilized on the CM5 sensor chips. The final amounts of immobilized his-rTcHpHbR and his-rTbHpHbR were 800 RU and 480 RU, respectively. The dissociation constants (K_d) were calculated by the kinetics analysis, using a BIAevaluation software (BIACORE Co., Ltd. Tokyo, Japan).

5-3. Results

Cloning and sequencing of *tchphbr* and *tbhphbr*

The truncated *tchphbr* was PCR-amplified from TcIL3000 gDNA, based on the reported sequence (Gene ID: TcIL3000.10.2930). In order to determine the copy number of the *tchphbr* in the genome of TcIL3000, a Southern blot analysis was performed. In single-digestion of the *tchphbr* with *Nsi*I or *Sac*II, case three signals were observed in each with a common 1,800-bp signal (Fig. 5A, lanes 1 and 2). Upon *Pst*I treatment, which cut the flanking region of the *tchphbr*, only two signals (3,400 bp and 15,900 bp) were observed (Fig. 5A, lane 3). These results indicated that *tchphbr* was a two-copy gene as shown in the gene map (Fig. 5B). The determined DNA sequence of TcHpHbR (Accession No. LC190899) showed 18 base-substitution compared with the reference alignment of TcHpHbR (data not shown). And the translated AA sequence from the LC190899 showed 7 AA substitutions, as compared with the reference alignment of TcHpHbR (Fig. 6A, V28A, A34G, A86V, N94D, A134V, T138V and N153D). On the other hand, the determined AA sequence of TbHpHbR was completely consistent with the reference alignment of TcHpHbR (Fig. 6B). The determined AA sequence of TcHpHbR displayed 30% identity with TbHpHbR (Fig. 6C). As the results of the structure-prediction of TcHpHbR and TbHpHbR, both of them were consisted primarily of a three-helical bundle (data not shown).

The expression profile of TcHpHbR

In order to examine the expression profile of TcHpHbR during the life cycle of

the parasite, northern blotting, western blotting and confocal laser scanning microscopic analyses were performed. Northern blotting analysis revealed that the transcription of TcHpHbR mRNA (2 kb) was exclusively occurred in the EMF stage of the parasite (Fig. 7A, lane 3). In western blotting analyses, the TcHpHbR protein was detected as 42-kDa and 37-kDa proteins in the EMF and MCF stages (Fig. 7B, lanes 3 and 4), although the signals in the MCF were weaker than that in EMF. To analyze the cellular localization of TcHpHbR in the parasite, each life cycle stage of the parasite (from *in vitro* cultures) was incubated with α-rTcHpHbR mouse immune sera, and examined in confocal laser scanning microscopy. Consistent with the results of the northern and western blot analyses, the cell surface and cytosol of EMF stage parasite was specifically stained by the polyclonal antibody (Fig. 7C). Especially, the signal of TcHpHbR was strong near the flagellar pocket of EMF (Fig. 7C, (3 and 3'), arrow head).

Hemoglobin uptake in *T. congolense*

To clarify the Hb uptaking in *T. congolense*, the uptake of free-Hb^{A488}, free-Hp^{A488} or Hp^{A488}Hb complex was examined in each life cycle stage of the parasite (Fig. 8). Endocytic compartments (endosome, flagellar pocket and lysosomes) were also visualized as red spots using biotinylated tomato lectin and fluorochrome-labeled streptavidin. The EMF-specific uptake of free-Hb^{A488} was visualized as green spots indicated by arrows closed to the nucleus and kinetoplast of parasite (Fig. 8, EMF panel of the first row). In addition, the free-Hb^{A488} (green spot) was found to co-localization with biotinylated tomato lectin (red spot), a marker for endocytic compartments, in only

the EMF parasites. On the other hand, no detectable signals of free-Hp^{A488} and Hp^{A488}Hb complex uptake were observed in any developmental stages of the parasite (Fig. 8, panels of the second and third rows).

Direct interactions of TcHpHbR and free-hemoglobin components

The direct interaction of TcHpHbR and free-Hb was qualitatively examined by a GST pull-down assay. Free-Hb purified from bovine RBCs occurred as 25.8-kDa Hb dimer and as 12.8-kDa α-subunit and 13.2-kDa β-subunit (Fig. 9, lane 1). On the other hand, the GST-rTcHpHbR was observed to have an expected molecular mass of 64 kDa (Fig. 9, lanes 2-4), while that of GST was 25 kDa (Fig. 9, lanes 5-7). When the GST-rTcHpHbR was incubated with 2 mg/mL of free-Hb, Only the α- and β-subunits of Hb were co-precipitated (Fig. 9, lanes 2). In addition, the 12.8-kDa α-subunit and a 13.0-kDa γ-subunits of fetal Hb were co-precipitated, when the GST-rTcHpHbR was incubated with FBS (Fig. 9, lane 3). In contrast, GST did not interact with any Hb (Fig. 9, lanes 5-6).

Investigation of the specific ligand of TcHpHbR

To compare the binding affinity of TcHpHbR with that of TbHpHbR, SPR assays were performed. The results showed that the rTbHpHbR had a low binding affinity for both free-Hp (K_d = 1.8 μM) and free-Hb (K_d = 5.3 μM) (Fig. 10A, panels (1) and (2)). In contrast, the rTcHpHbR displayed a high affinity for both the free-Hp and free-Hb (Fig. 10A, panels (3) and (4)). However, the affinity of rTcHpHbR for free-Hb (K_d =

20.5 nM) was 10-times higher than that for free-Hp (K_d = 220 nM). These results indicated that free-Hb was possibly a specific ligand for the rTcHpHbR, while both the free-Hb and free-Hp were not specific ones for the rTbHpHbR. Our findings were consistent with the previous report that TbHpHbR displayed a high affinity for HpHb (138), because the RUs increased in proportion to the amount of free-Hp against free-Hb (Fig. 10B, panel (1)). In other words, when the amount of free-Hp against free-Hb was increased, the amount of HpHb was also Hp increased, depended on the Hp dose. In contrast, for rTcHpHbR, the RUs decreased inversely and proportionally, to the amount of free-Hp against free-Hb (Fig. 10B, panel (3)), indicating that the amount of free-Hb bound was decreased due to the increased amount of HpHb complex. The RUs of both TbHpHbR and TcHpHbR were increased due to the increase of the amount of free-Hb against free-Hp (Fig. 10B, panels (2) and (4)).

5-4. Discussion

Unlike other eukaryotes, trypanosomes obtain heme sources extracellularly, because they lack a pathway for heme synthesis (14). As seen in *Trypanosoma* and *Leishmania,* heme uptake is important for the growth and development of the parasites (2, 138). For example, TbHpHbR knockout mutants caused a decrease in the proliferation rate of *T. brucei* in the infected mice (138). In contrast to the mammalian life cycle stage of trypanosomes, the vector life cycle stages of trypanosomes require much higher amounts of heme, because they need to produce many heme proteins for an active electron transport chain mitochondrial respiration in the stages (17, 18, 85). Thus, Hb uptake via Hb receptors has been suggested to be more essential for the survival of the vector life cycle stages than that of mammalian stage in *Trypanosoma* parasites. Nevertheless, the mechanisms, by which the vector life cycle stages of African trypanosomes, such as the PCF and EMF, take up the heme, have not been examined well.

In chapter I, I examined the expression profile, binding specificity and binding parameters of TcHpHbR, which had previously been reported as a *T. congolense* orthologue of *tbhphbr* (138). Although the *tbhphbr* had ever been described as a single copy gene, our work showed that it was a two copy-gene with a tandem arrangement. The AA sequences of TcHpHbR and TbHpHbR indicated that they shared 30% identity. Previously, Higgins *et al*. (2013) reported that TcHpHbR was structurally similar to two well-characterized trypanosome GPI-anchored surface proteins (namely, VSG MITat 1.2 and glutamic acid/alanine-rich protein) in terms of their characteristic three-helical

bundle (59). Note that, the seven AA substitutions between the determined AA sequence and reference AA sequence of TcHpHbR displayed similar properties. Because of the similarity of these substitutions, the three-dimension structure of obtained TcHpHbR could be highly conserved. The result of structure prediction of TcHpHbR supported this speculation (data not shown). Additionally, the core AAs were completely conserved that contributed to the interaction between TcHpHbR and free-Hb (75). Thus, I concluded that these substitutions did not abolish the three-dimension structure and biological function of TcHpHbR.

Next, *tchphbr* was exclusively transcribed and translated as 37-kDa and 42-kDa proteins in the EMF of *T. congolense* in protein expression analysis. Presumably, the 37-kDa protein was an unmodified form of TcHpHbR without the N-terminal signal peptide (Met_1 to Val_{37}), while the 42-kDa protein was suggested to be a post-translationally modified TcHpHbR. The molecular mass of TcHpHbR was similar to the predicted molecular mass of TbHpHbR (43.3 kDa), the apparent mass of which was 72 kDa because of N-glycosylation (138). Thus, TcHpHbR might be expressed with fewer post-translational modifications than TbHpHbR. It was reported that TcHpHbR was structurally truncated as compared to TbHpHbR, presumably, because the TcHpHbR does not need to protrude above a VSG layer, which is absent on the cell surface of EMF parasites (59). These differences between TcHpHbR and TbHpHbR might be related to their different expression profiles during the parasites life cycle.

Unlike TbHpHbR, the cellular localization of TcHpHbR was not limited to the flagellar pocket, rather it was expressed throughout the entire surface of EMF cells.

However, since the Hb uptake should occur through the flagellar pocket (44), the TcHpHbR located on the cell surface seemed to translocate to the flagellar pocket when it has bound Hb. Weak signals of TcHpHbR were also observed in MCF in the western blot analyses. The result of proteome analysis throughout the life cycle of *T. congolense* showed that the expression level of TcHpHbR in MCF was 11~17% as compared with in EMF (46). I considered that the weak signals in MCF were due to the result of the miner population of MCF, which had differentiated immediately from EMF, because the RNA transcription of TcHpHbR was undetectable in northern blot analysis.

The ligand specificity of TcHpHbR was also different from that of TbHpHbR. TbHpHbR was an Hp-Hb complex-specific receptor (59, 138), whereas TcHpHbR bound free-Hb with a high affinity. The ligand-binding characteristics of TcHpHbR and TbHpHbR were differed when the amount of free-Hp was exchanged against the specific amount of free-Hb (50 μg/mL). It suggested that the majority of free-Hb molecules might not form the HpHb complex in the tsetse midgut due to a lack of sufficient amount of Hp molecules, where excessive amount of Hb would be released from digested RBCs in tsetse midgut. The different ligand specificity between TcHpHbR and TbHpHbR might have evolved as a consequence of adaptation of the different life cycle stages of the two species to their different parasitism within their vector (57). Since *T. congolense* EMF occupies in the proboscis at the tsetse fly vector (99), it seems that they are periodically exposed to a high level of free-Hb during blood meals. Hence, *T. congolense* EMF may effectively take up the free-Hb by using the specific receptor, TcHpHbR. In contrast, *T. brucei* EMF inhabit in the salivary glands of

their tsetse fly vector (109). Thus, the parasites do not come in contact with free-Hb.

In this study, the Hb accumulation in flagellar pocket could not be observed in *T. congolense* BSF, PCF and MCF stages. On the other hand, *T. congolense* BSF and PCF parasites could proliferate stably *in vitro* culture and *in vivo*, in spite of the requirement of heme for surviving (141). These findings suggested that *T. congolense* BSF and PCF might have unknown heme-source uptake mechanisms other than Hb and HpHb. Further studies are needed in order to clarify the mechanisms.

In conclusion, I revealed that TcHpHbR, a TbHpHbR orthologue in *T. congolense*, was EMF-specific, free-Hb receptor. I, therefore, propose that the TcHpHbR should be renamed as *T. congolense* epimastigote-specific free-Hb receptor (TcEpHbR).

Table 1. Primers used in this chapter

Primer name	Sequence (5'-3')	Usage
TcHpHbR-SG F	GGATCC*GCTGAAGGAGAGATCAAGGT	• Gene cloning • DNA probe for TcHpHbR detection in Southern and northern blot
TcHpHbR-SG R	GCGGCCGC**TGAGGATTCTGTCTCAACCT	
TbHpHbR-SG F	GGATCC*GCTGAGGGTTTAAAAACCAA	• Gene cloning
TbHpHbR-SG R	GCGGCCGC**ACTAACCACGTCAACGGGCCT	
18s rRNA F	GATCTGGTTGATTCTGCCAG	• DNA probe for 18s rRNA detection as internal reference in northern blot
18s rRNA R	AAATGAGCCAGCTGCAGGTTC	

Under lines indicate restriction enzyme sites: **Bam*HI, ***Not*I

18s rRNA primers were referred from Suganuma *et. al.*, 2013 (128).

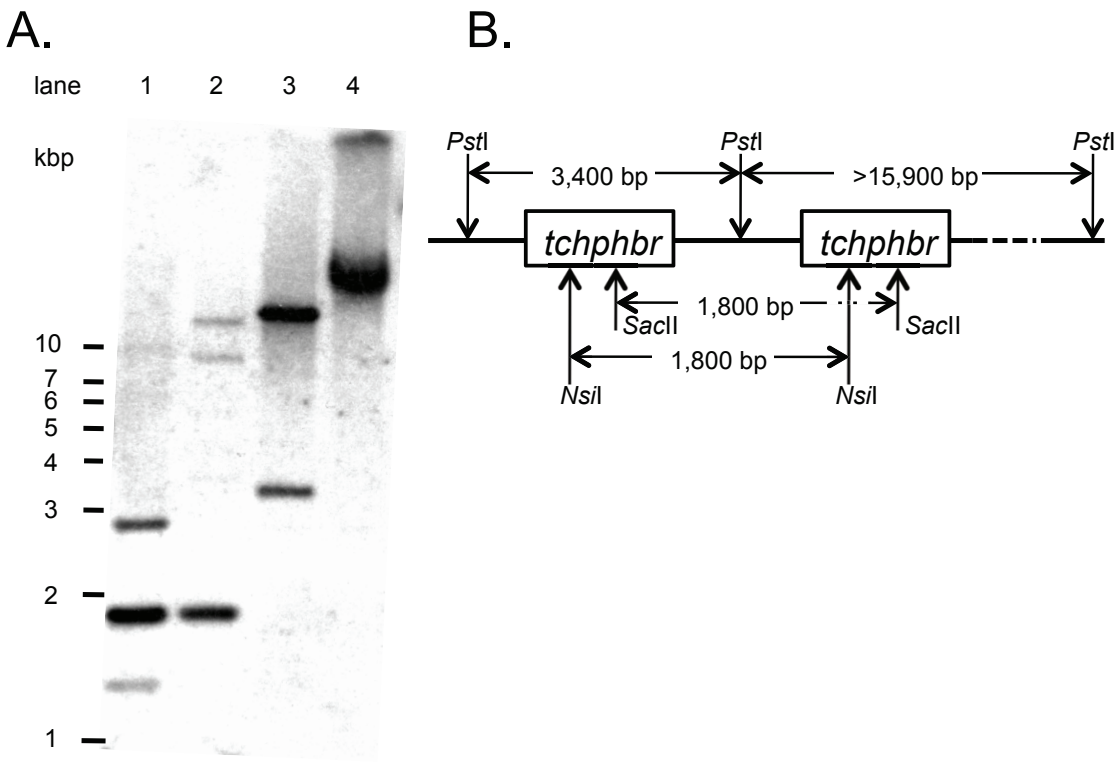

Fig. 5. Southern blot analyses. A: Southern blot analyses of the *tchphbr*. TcIL3000 gDNA treated with *Nsi*I (lane 1), *Sac*II (lane 2), *Pst*I (lane 3) or neat TcIL3000 gDNA (lane 4) was subjected to Southern blot analyses. **B:** The predicted genome organization and its restriction map of *tchphbr*.

A.

```
TcHpHbR              ----------------------AEGEIKAELKDGDEVAAACELRAQLAGVSIASGILLRP 38
TcIL3000.10.2930     MRFALLLLCASLLCRASLAQVVAEGEIKVELKDADEVAAACELRAQLAGVSIASGILLRP 60
                                           ******.****.**************************

TcHpHbR              AVIRNATTEFSRKKSEEILAKGGAAVERASAAVDRVSGLDKANETAQKVRKAAAVAHHAL 98
TcIL3000.10.2930     AVIRNATTEFSRKKSEEILAKGGAAAERASAAVNRVSGLDKANETAQKVRKAAAVAHHAL 120
                     ************************.*******:**************************

TcHpHbR              EHVKEEVEIVAKKVNEIVELTAGATEHAKGAKSNGDASVVKVSNLLARAKESEDQYVKKA 158
TcIL3000.10.2930     EHVKEEVEIVAKKANEITELTAGATEHAKGAKANGDASVVKVSNLLARAKESEDQYVKKA 180
                     *************.***.**************:**************************

TcHpHbR              AEECSNSTNYDVTAKSLAAALDKLPGVKEDNAVKTTFQSILTSLDNLDKDVKSVEQRAEE 218
TcIL3000.10.2930     AEECSNSTNYDVTAKSLAAALDKLPGVKEDNAVKTTFQSILTSLDNLDKDVKSVEQRAEE 240
                     ************************************************************

TcHpHbR              LETALEKAERQLEKAEKAAEEAETESSKVETESS---------------------- 252
TcIL3000.10.2930     LETALEKAERQLEKAEKAAEEAETESSKVETESSTSCPVAVSALLLMGTVAIYAGF 296
                     ********************************
```

Fig. 6. The AA alignment of TcHpHbR, TcIL3000.10.2930 and Tb927.6.440.

A: Alignment of the AA sequence of TcHpHbR that was cloned in this study, with that of the TcIL3000.10.2930 that was obtained from a TritrypDB database as the reference. The conserved residues are shown as: fully conserved (*), strongly conserved (:) and weakly conserved (.). Red indicated the AAs that form the core of the interaction between TcHpHbR and HpHb (75).

B.

```
TbHpHbR          -----------------------------------AEGLKTKDEVEKACHLAQQLKEVSI 25
Tb927.6.440      MEKPSCRGAGWAQLLWCYGTCCALLLRLIVEASQAAEGLKTKDEVEKACHLAQQLKEVSI 60
                                                    *************************

TbHpHbR          TLGVIYRTTERHSVQVEAHKTAIDKHADAVSRAVEALTRVDVALQRLKELGKANDTKAVK 85
Tb927.6.440      TLGVIYRTTERHSVQVEAHKTAIDKHADAVSRAVEALTRVDVALQRLKELGKANDTKAVK 120
                 ************************************************************

TbHpHbR          IIENITSARENLALFNNETQAVLTARDHVHKHRAAALQGWSDAKEKGDAAAEDVWVLLNA 145
Tb927.6.440      IIENITSARENLALFNNETQAVLTARDHVHKHRAAALQGWSDAKEKGDAAAEDVWVLLNA 180
                 ************************************************************

TbHpHbR          AKKGNGSADVKAAAEKCSRYSSSSTSETESQKAIDAAANVGGLSAHKSKYGDVLNKFKLS 205
Tb927.6.440      AKKGNGSADVKAAAEKCSRYSSSSTSETESQKAIDAAANVGGLSAHKSKYGDVLNKFKLS 240
                 ************************************************************

TbHpHbR          NASVGAVRDTSGRGGKHMEKVNNVAKLLKDAEVSLAAAAAEIEEVKNAHETKVQEEMKRN 265
Tb927.6.440      NASVGAVRDTSGRGGKHMEKVNNVAKLLKDAEVSLAAAAAEIEEVKNAHETKVQEEMKRN 300
                 ************************************************************

TbHpHbR          GNPIENESETNSGGNAESQGNGDREDKNDEQQQVDEEETKVENGSSEEGSCCGNESNGPH 325
Tb927.6.440      GNPIENESETNSGGNAESQGNGDREDKNDEQQQVDEEETKVENGSSEEGSCCGNESNGPH 360
                 ************************************************************

TbHpHbR          VMKKRHGVGAPRPVDVVS------------------------- 343
Tb927.6.440      VMKKRHGVGAPRPVDVVSGFRSYASASFALLSLVRVGILQVVV 403
                 ******************
```

B: The alignment of the AA sequences of TbHpHbR that was cloned in this study, with that of Tb927.6.440 that was obtained from the TritrypDB database as the reference. The conserved residues are shown as: fully conserved (*).

C.

```
TcHpHbR          ------------------------------AEGEIKAELKDGDEVAAACELRAQLAGVSI 30
Tb927.6.440      MEKPSCRGAGWAQLLWCYGTCCALLLRLIVEASQAAEGLKTKDEVEKACHLAQQLKEVSI 60
                                               .:    **  ***  **.*  **  ***

TcHpHbR          ASGILLRPAVIRNATTEFSR---KKSEEILAKGGAAVERASAAVDRVSGLDKANET-AQK 86
Tb927.6.440      TLGVIYRTTERHSVQVEAHKTAIDKHADAVSRAVEALTRVDVALQRLKELGKANDTKAVK 120
                 : *:: *.:  :.. .*  :   .*  : :::.  *: *...*::*:. *.***:* * *

TcHpHbR          VRKAAAVAHHALEHVKEEVEIVAKKVNEIVELTAGATEHAKGAKSNGDASVVKVSNLLAR 146
Tb927.6.440      IIENITSARENLALFNNETQAVLTARDHVHKHRAAALQGWSDAKEKGDAAAEDVWVLLNA 180
                 : :  : *:. *  .::*.: * .  :.: :  *.* :  ..**.:***:. .*  **

TcHpHbR          AKESE-DQYVKKAAEECSNSTNYDVTAKSLAAALDKLPGVKEDNAVKTTFQSILTSLDNL 205
Tb927.6.440      AKKGNGSADVKAAAEKCSRYSSSSTSETESQKAIDAAANVGGLSAHKSKYGDVLNKFKLS 240
                 **:.: .  ** ***:**. :. ..: ..   *:*  ..*   .* *:.: .:*..:.

TcHpHbR          DKDVKSVEQR-----------------AEELETALEKAERQLEKAEKAAEEAETESSK-- 246
Tb927.6.440      NASVGAVRDTSGRGGKHMEKVNNVAKLLKDAEVSLAAAAAEIEEVKNAHETKVQEEMKRN 300
                 : .* :*.:                   :: *.:*  *  ::*:.::* *    *. *

TcHpHbR          ---VETESS---------------------------------------------------- 252
Tb927.6.440      GNPIENESETNSGGNAESQGNGDREDKNDEQQQVDEEETKVENGSSEEGSCCGNESNGPH 360
                    :*.**.

TcHpHbR          -------------------------------------------
Tb927.6.440      VMKKRHGVGAPRPVDVVSGFRSYASASFALLSLVRVGILQVVV 403
```

C: The alignment of the AA sequences of TcHpHbR that was cloned in this study, with that of Tb927.6.440 that was obtained from the TritrypDB database as the reference. The conserved residues are shown as: fully conserved (*), strongly conserved (:) and weakly conserved (.).

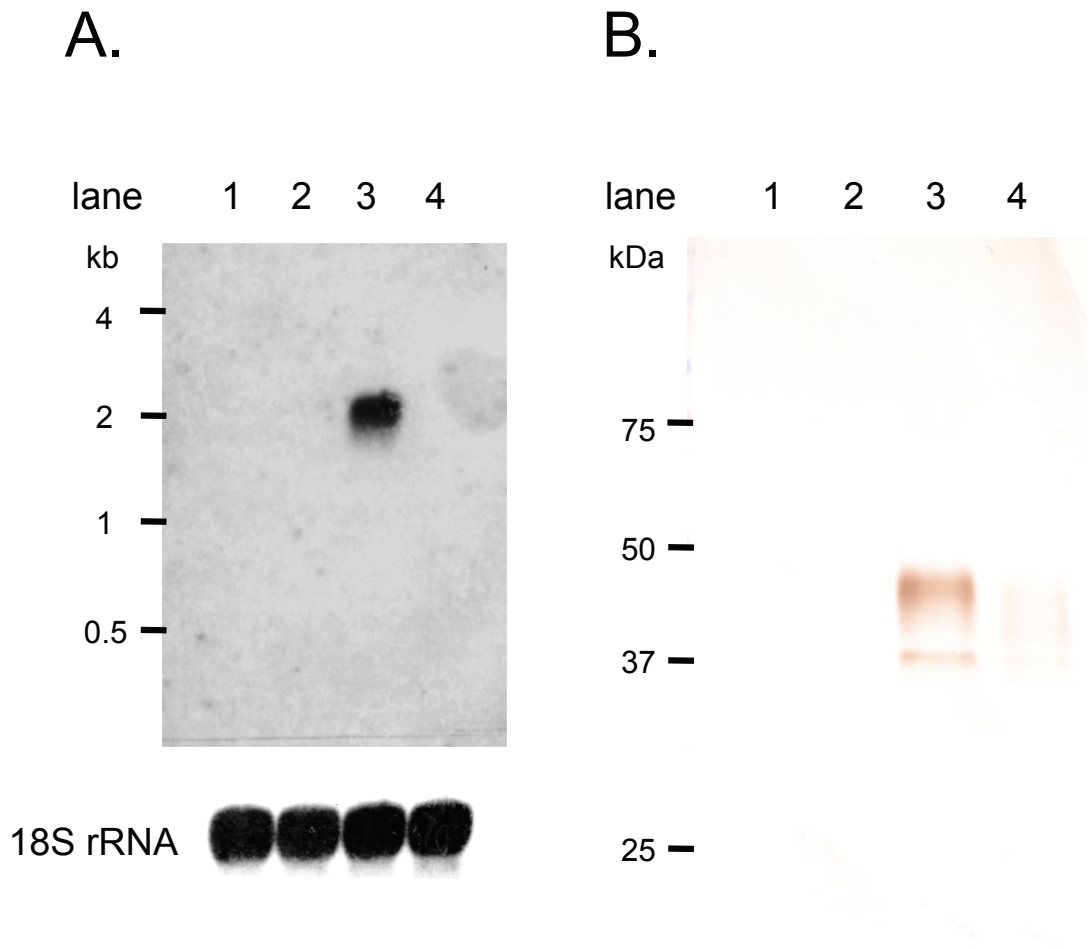

Fig. 7. Expression profile of TcHpHbR. A: The TcHpHbR mRNA expression profile was examined by northern blot analysis. Total RNA extracted from TcIL3000 BSF (lane 1), PCF (lane 2), EMF (lane 3) and MCF (lane 4) were used for the analysis. The DNA probe to detect TcHpHbR mRNA was prepared by a PCR using the primers (18s rRNA F and 18s rRNA R) shown in Table 1. 18S rRNA was used as an internal reference. **B**: The TcHpHbR protein expression profile was examined by western blotting analysis. Total proteins (2 μg/lane) extracted from TcIL3000 BSF (lane 1), PCF (lane 2), EMF (lane 3) and MCF (lane 4) were analyzed by western blotting using α-rTcHpHbR mouse immune sera.

C.

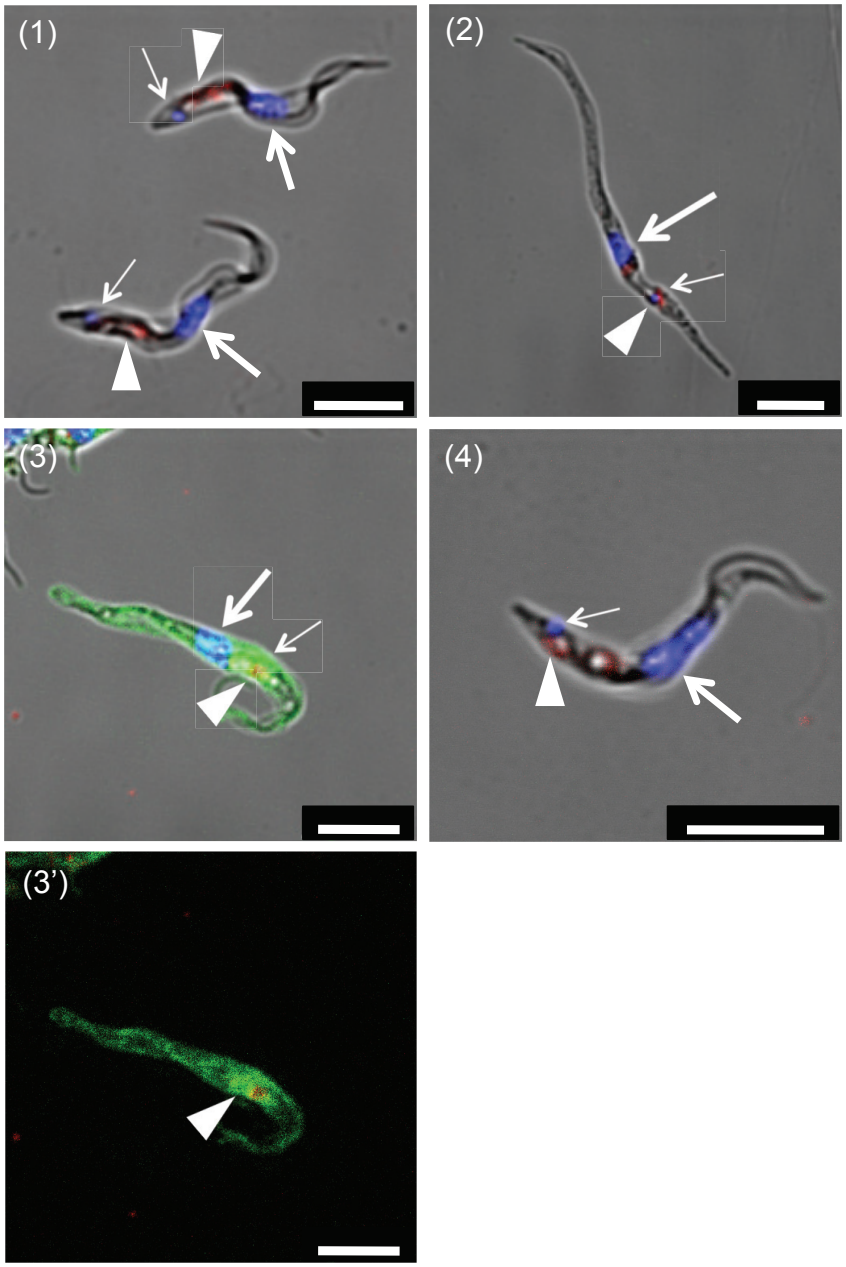

C: The cellular localization of TcHpHbR in TcIL3000 BSF (1), PCF (2), EMF (3) and MCF (4) was examined in an indirect immunofluorescence assay (IFA) using anti-rTcHpHbR mouse sera. The signals of TcHpHbR and endocytic compartments were abstracted from (3) panel for focus on the co-localization of TcHpHbR and endocytic compartment (3'). The green, blue and red signals indicate TcHpHbR, DNA (bold arrow: nucleus, fine arrow: kinetoplast) and the endocytic compartment (arrowhead), respectively. Bar = 5 μm

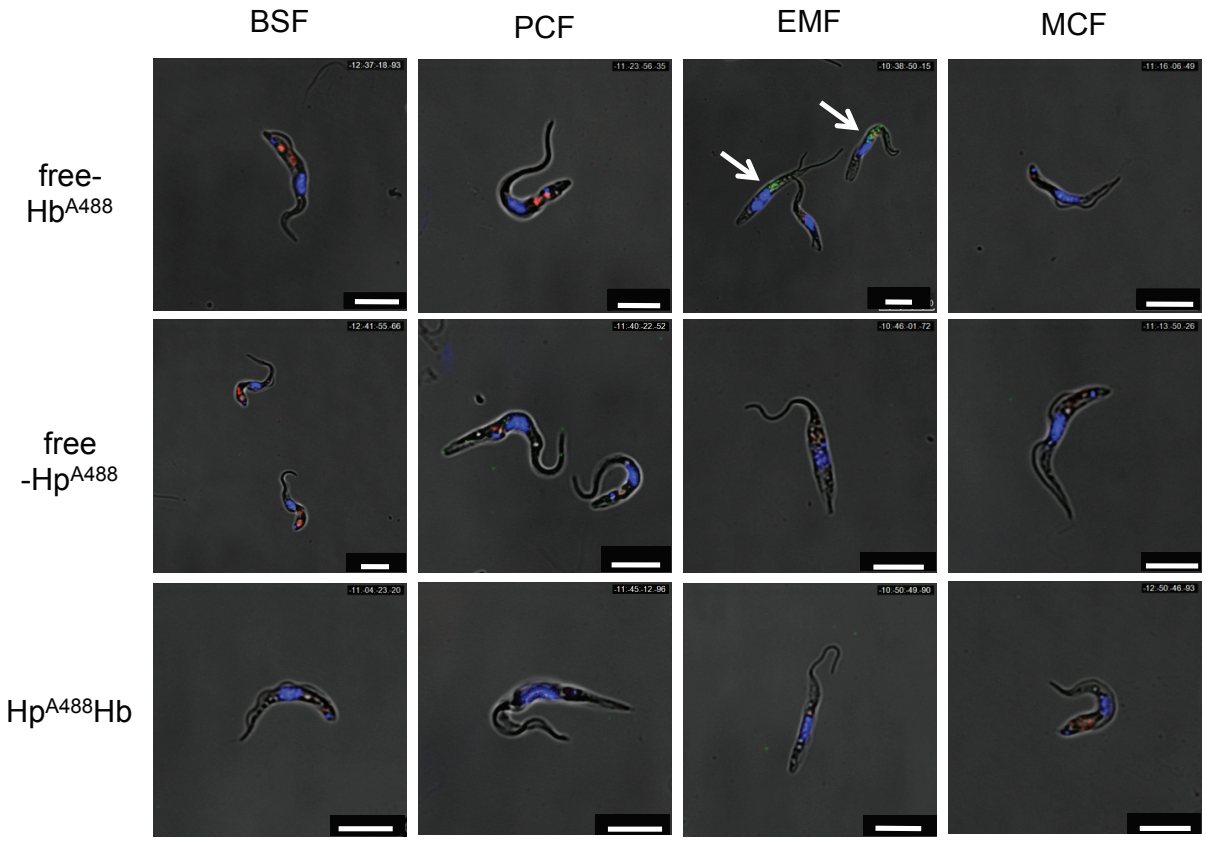

Fig. 8. Comparison of hemoglobin uptake throughout the life-cycle stages of the parasite. The lysosomal accumulation of free-Hb^{A488}, free-Hp^{A488} or Hp^{A488} Hb complex was examined throughout the stages of the TcIL3000 life-cycle. The green, blue and red signals indicate Alexa 488-labelled proteins, DNA (nucleus and kinetoplast) and the endocytic compartment (flagellar pocket and lysosome), respectively. The arrows indicate the accumulation of free-Hb^{A488} in the endocytic compartment in EMF. Bar = 5 μm

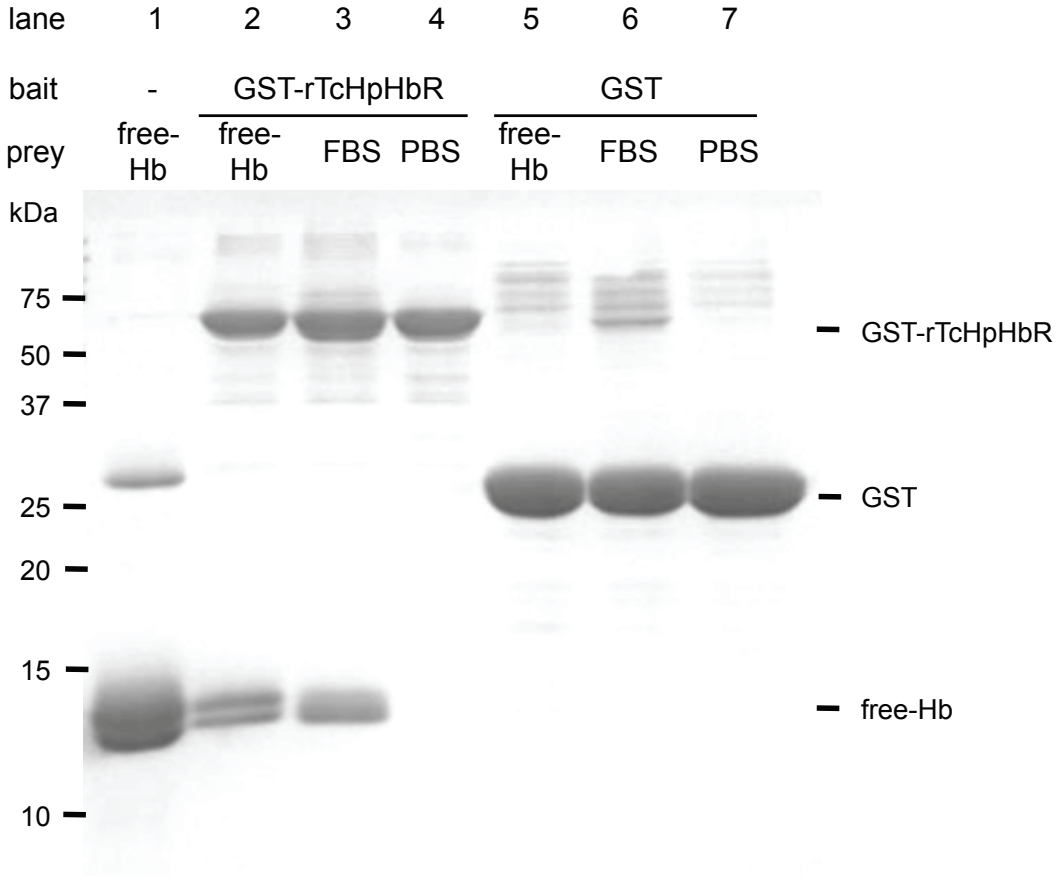

Fig. 9. Assessment of qualitative binding between rTcHpHbR and free-Hb by a pull-down assay. The qualitative interaction between rTcHpHbR and free-Hb was analyzed by a pull-down assay using glutathione sepharose beads. Free-Hb (lane 1), GST-rTcHpHbR (lane 4) and GST (lane 7) were used as the size standards of each protein. GST-rTcHpHbR (lanes 2-4) and GST (lanes 5-7) were used as bait proteins. Free-Hb (lanes 2, and 5) and diluted FBS (lanes 3 and 6) were used as prey proteins.

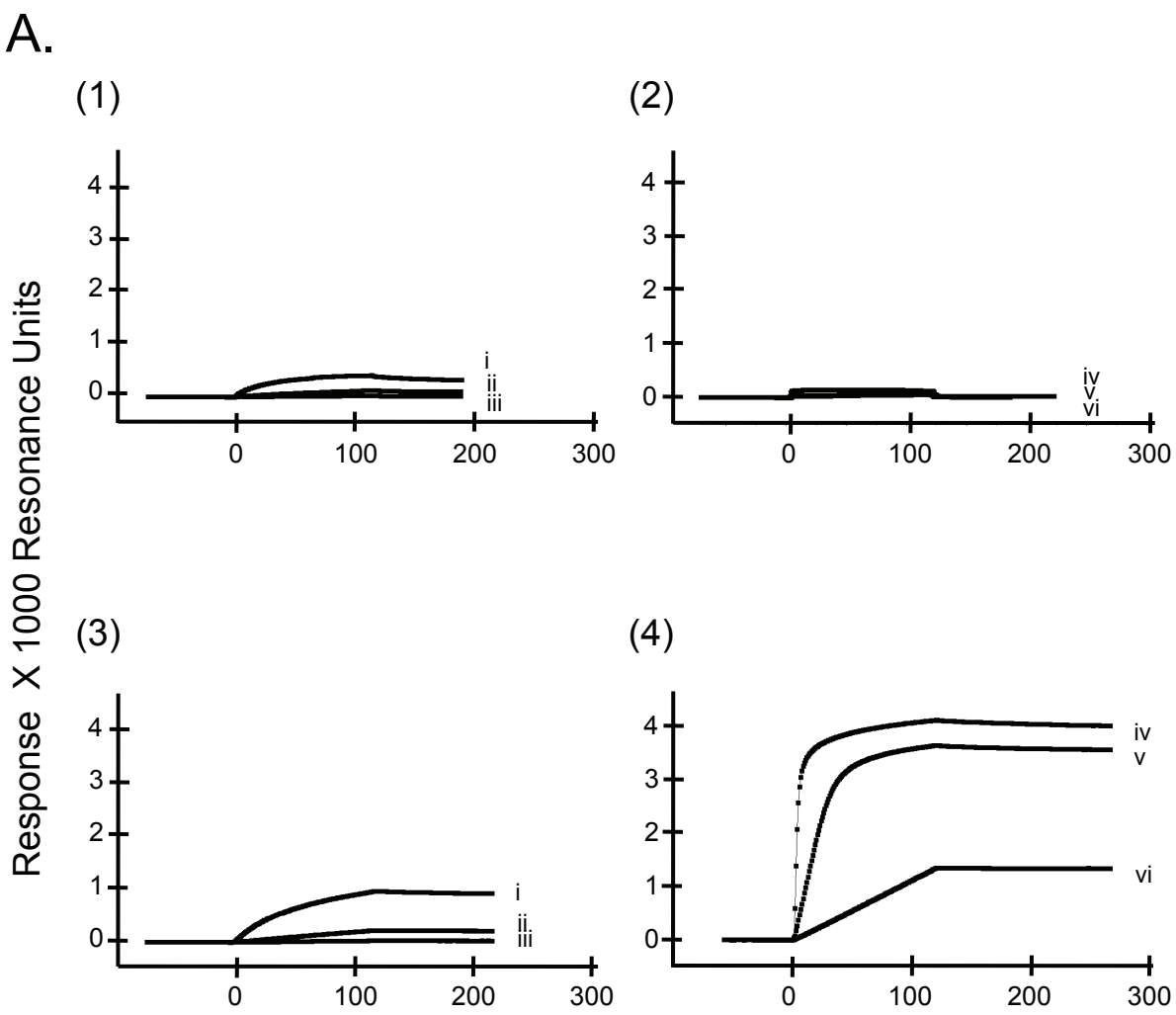

Fig. 10. SPR assays of rTcHpHbR and rTbHpHbR. The quantitative binding assays of his-rTcHpHbR and his-rTbHpHbR were performed in SPR assays. The vertical axis shows the binding response (RU), while the horizontal axis shows the running time (in seconds). His-rTcHpHbR or his-rTbHpHbR were used as the immobilized receptor. **A:** The interactions were analyzed between his-rTbHpHbR and free-Hp (1), his-rTbHpHbR and free-Hb (2), his-rTcHpHbR and free-Hp (3), his-rTcHpHbR and free-Hb (4). The concentrations of used analytes were as follows: free-Hp 100 μg/mL (i), 10 μg/mL (ii), 1 μg/mL (iii) and free-Hb 100 μg/mL (iv), 10 μg/mL (v), 1 μg/mL (vi).

B.

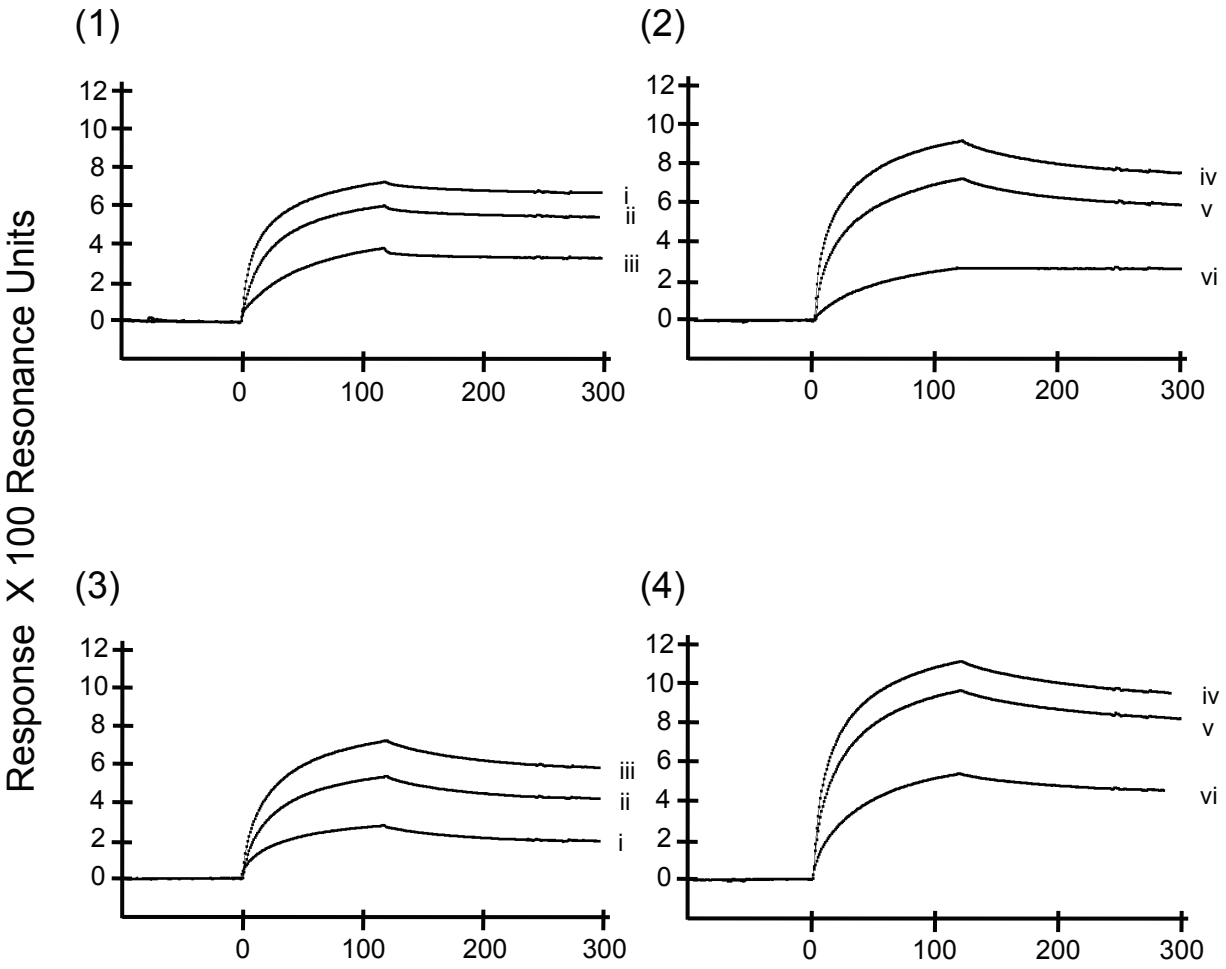

B: The interaction between the HpHb complex and his-rTbHpHbR ((1) and (2)) or his-rTcHpHbR ((3) and (4)). The concentrations of used analytes were as follows: Hp 100 µg/mL and Hb 50 µg/mL (i), Hp 50 µg/mL and Hb 50 µg/mL (ii and v), Hp 10 µg/mL and Hb 50 µg/mL (iii), Hp 50 µg/mL and Hb 100 µg/mL (iv), Hp 50 µg/mL and Hb 10 µg/mL (vi).

6. CHAPTER II

Effect of anti- *Trypanosoma congolense* epimastigote-specific free-Hb receptor antibodies against *T. congolense* epimastigote forms

6-1. Introduction

In chapter I, I revealed a novel Hb receptor, namely *Trypanosoma congolense* epimastigote-specific hemoglobin receptor (TcEpHbR), which was only expressed in epimastigote (EMF) of *T. congolense.* This receptor is the first hemoglobin (Hb) receptor found in *T. congolense*. The chapter I also showed unique ligand-binding affinity, which was a different life stage-specific pattern from the orthologue of *T. brucei* (75, 144).

In this chapter, I aimed to evaluate the possibility of TcEpHbR as a candidate of transmission blocking vaccine (TBV) molecule. Considering the necessity of heme for trypanosome survival, Hb taken up via TcEpHbR might be an essential step for the EMF. Because the growth of TbHpHbR-knock down *T. brucei* bloodstream form (BSF) was attenuated in the mouse infection model (138), a strategy of the interference to TcEpHbR with anti-TcEpHbR antibody was hypothesized as a novel trypanosome control strategy. In order to evaluate the possibility of TcEpHbR as a TBV target, anti-TcEpHbR polyclonal and monoclonal antibodies (mAb) were assessed for their trypanocidal effects against *T. congolense* EMF *in vitro*.

6-2. Materials and methods

Trypanosomes and culture conditions

T. congolense IL3000 (TcIL3000) strain EMF was maintained *in vitro* as described in chapter I.

Production and purification of monoclonal antibodies

Sp2/0Ag4 myeloma cells were maintained in 5% fetal bovine serum (FBS)-supplemented GIT medium (Wako Pure Chemicals Industries Ltd.) at 37ºC in 5% CO_2. Five BALB/cAJcl seven-weeks-old female mice (CLEA Japan, Inc.) were immunized with the his-tagged recombinant TcEpHbR (his-rTcEpHbR) as described in chapter I. After four-time immunizations, 50 μL of his-rTcEpHbR solution was injected to mice by intravenous injection through their tail vains. Next day, the mice were sacrificed under a terminal anesthesia, and the spleens were sampled. The splenocytes were aseptically collected from these spleens, while Sp2/0Ag4 myeloma cells were harvested from the maintained culture (35). The collected splenocytes and Sp2/0Ag4 myeloma cells were mixed in a cell number ratio of 5:1, and then fused by polyethylene glycol method (119). Fused cells were spread in the hybridoma selective medium that composed of GIT supplemented 0.7% methylcellulose (Thermo Fisher Scientific, MA, U. S. A.) and hypoxanthine-aminopterin-thymidine (CORNING, NY, U. S. A) (119). The colonies of hybridoma cells were picked up from the selective GIT medium, and isolated into each well of 96-well plate. After five-day incubation in the selective GIT media, mAb-producing hybridoma clones were screened by using an enzyme-linked

immunosorbent assay (ELISA), and the antibody activities were evaluated by western blot analysis and indirect immunofluorescence assay (IFA).

The antibodies that were contained in the hybridoma supernatants were concentrated by ammonium-sulfate precipitation and purified by a column chromatography of protein G. First, the antibodies were salted out by saturated ammonium sulfate (SAS) and dialyzed five times by serial diluted SAS with PBS. After the dialysis, the antibodies were purified by using protein-G column-chromatography kit (GE Healthcare Corp.), following the manufacture's instruction. After purification, the antibodies were isotyped by using isotyping kit (Roche Diagnostics K. K.).

Enzyme-linked immunosorbent assay (ELISA)

The his-rTcEpHbR was dialyzed against phosphate-buffered saline (PBS), and diluted with 0.05 M carbonate-bicarbonate buffer at pH 9.6 to a final concentration of 200 ng/mL. One hundred microliters of the his-rTcEpHbR solution were coated on a 96-well microplate (Nunc, Roskilde, Denmark) at 4ºC for over night after 2-h incubation at 37ºC in a moisture box. After washing three times with PBS containing 0.05 % Tween 20 (PBS-T), the plate was blocked with 1% bovine serum albumin (BSA) in PBS for 1 h at room temperature (RT). The plate was washed three times with PBS-T, and 100 μL of 1:5 diluted hybridoma culture supernatants with PBS were applied to each well. The plate was incubated for 1 h at 37ºC, and washed 10 times with PBS-T, and then 100 μL of horseradish peroxidase (HRP)-conjugated anti-mouse IgG (GE Healthcare Bio-Sciences Corp., U. K.) at a dilution of 1:2,500 with 1% BSA in

PBS were added to each well. The plate was incubated for 1 h at 37ºC, and washed 10 times with PBS-T. Then, 100 μL of substrate solution (TMB, Kirkegaad & Perry Laboratories, Baltimore, U. S. A.) was added to each well. After 5-min incubation at RT, the reaction was terminated by adding 100 μL of 1 M phosphoric acid into each well. The absorbance at 450 nm was measured by a microplate reader (MTP-500, CORONA ELECTRICS Co.,Ltd., Ibaraki, Japan).

Western blot analysis

Total proteins of EMF were used as antigen, as seen in chapter I. The protein extracts (2 μg) were separated by 10% sodium dodecyl sulfate-polyacrylamide gel electrophoresis (SDS-PAGE), and electrophoretically transferred onto a polyvinylidene difluoride (PVDF) membrane (GE Healthcare Bio-Sciences Corp.). After blocking with 5% skim milk in PBS at RT for 1 h, the blotted membrane was incubated with the 1:5 diluted supernatant from each hybridoma culture with PBS or with 1:1,000 diluted α-rTcEpHbR mouse immune sera as 1st antibody at 27ºC for 1 h. The membranes were washed three times with PBS-T, and then incubated with 1:2,500 diluted anti-mouse IgG conjugated with HRP at 27ºC for 1 h. After wash with PBS-T for three times, the signals were detected by a 3, 3'-diaminobenzidine (DAB, Sigma-Aldrich Co., MO, U. S. A.) detection system.

Indirect immunofluorescence assay (IFA)

The EMF parasites were collected from the supernatant of EMF culture, and washed three times with PBS. The EMF cells were suspended in the supernatants of mAb-producing hybridoma culture or in 1:100-diluted α-rTcEpHbR mouse immune serum, and then incubated for 1 h at 27ºC. After the incubation, EMF cells were washed with PBS for three times and resuspended with PBS. The EMF suspensions were spread over glass slides, air-dried and then fixed with 100% methanol. The specimens were incubated with 1:200-diluted anti-mouse IgG conjugated with fluorescein isothiocyanate (FITC, Thermo Fisher Scientific Inc.) and 20 μg/mL biotinylated tomato lectin (Vector Laboratories, Burlingame, U. S. A.). After three-time washes with PBS-T, the specimens were incubated with 30 μg/mL streptavidin conjugated with fluorochrome (Vector Laboratories). Nucleus and kinetoplast DNAs were stained with Hoechst 33342 (Dojindo, Kumamoto, Japan). A confocal laser scanning microscope was used to observe the prepared specimens.

Growth inhibition assay

The 1 x 10^5 parasites of EMF were inoculated in each well of a 96-well plate (Thermo Fisher Scientific) and pre-cultured in for 1 day at 27ºC. The adherent cells were washed with a flesh *T. vivax* medium-1 (TVM-1) to remove the non-adherent cells. Anti recombinant-TcEpHbR (α-rTcEpHbR) mAbs were diluted to 3 μg/mL, 15 μg/mL and 30 μg/mL with TVM-1. One hundred microliters of these mAb containing TVM-1 were added to each well of the EMF cultures, and the plate was incubated for 5 days at

27ºC. After the incubation, the plate was centrifuged at 2,000 rpm for 10 min at RT. The living EMF cells collected at the bottom of wells were morphologically observed by light microscopy, and assessed for their cell proliferation activities by a BrdU-uptake evaluation kit (Roche Diagnostics K. K.), following the manufacture's instruction.

Preparation of the truncated rTcEpHbRs

The truncated rTcEpHbRs were expressed in *E. coli* as GST-tagged protein as discribed in chapter I, and purified by using a glutathione sepharose beads column (GE Healthcare Bio-Sciences Corp.). The primers used in this chapter are shown in Table 2, and the truncated rTcEpHbR designs are shown in Fig. 9. The truncated GST-tagged rTcEpHbRs (GST-rTcEpHbRs) were cleaved from the GST-tag by a prescission protease buffer (50 mM Tris-HCl (pH. 7.0), 150 mM NaCl, 1 mM EDTA) containing 160 U/mL precision protease (GE Healthcare Bio-Sciences Corp.), and then dialyzed as described in chapter I. The truncated rTcEpHbRs were named as fragments A to I, and kept at -30ºC until use.

Epitope mapping by ELISA

The truncated and full length GST-rTcEpHbRs were dialyzed against PBS, and diluted with 0.05 M carbonate-bicarbonate buffer at pH 9.6 to a final concentration of 1 μg/mL. One hundred microliters of these recombinant protein solutions were coated on a 96-well microplate (Thermo Fisher Scientific) at 4ºC for overnight after 2-h incubation at 37ºC in a moisture box. After three-time washing with PBS-T, the plate

was blocked with 1% BSA in PBS for 1 h at RT. The plate was washed three times with PBS-T, and 100 μL of 1 μg/mL IgGs, which were purified from mAb-producing hybridoma cell culture supernatant, were applied to each well. The plate was incubated for 1 h at 37ºC, and washed 10 times with PBS-T, and then 100 μL of anti-mouse IgG conjugated with HRP at a dilution of 1:2,500 with 1% BSA in PBS were added to each well. The plate was incubated for 1 h at 37ºC, and washed 10 times with PBS-T. Then, 100 μL of TMB were added to each well. After 5-min incubation at RT, the reaction was terminated by adding 100 μL of 1 M phosphoric acid into each well. The absorbance at 450 nm was measured by the microplate reader.

The fragments H and I of truncated rTcEpHbR were coated on a 96-well microplate as described above. After washing three times with PBS-T, serially diluted guanidinium chloride (GnHCl, 1 M, 2 M, 4 M and 6 M) were added at 100 μL/well for antigen degeneration (103). After 1-h incubation at RT, the microplate was washed three times with PBS-T. Following ELISA steps (blocking, 1st antibody reaction, 2nd antibody reaction, HRP enzyme reaction and detection) were performed as described above.

Inhibition assay of hemoglobin uptake in *T. congolense* by supplementation with mAb

The EMF parasites were pre-incubated with TVM-1 on a four-well chamber slide (Thermo Fisher Scientific) for 1 day at 27ºC. After the pre-incubation, EMF cells were incubated in TVM-1 medium containing 15 μg/mL α-rTcEpHbR mAb for 15 min at

27ºC. After three-time washing with a fresh TVM-1, the EMF parasites were incubated with 20 μg/mL Hb^{A488} for 2.5 hs at 27ºC. Thereafter, the parasites were air-dried and fixed with 100% methanol for 10 min at RT. Nucleus and kinetoplast DNAs were stained with Hoechst 33342 for 30 min at 37ºC. After three-time washing with PBS-T, the intensities of fluorescence accumulation inside the EMF cells were measured by using a fluorescence microscope (BZ-9000, Keyence, Osaka, Japan) with the analyzing program (BZ analyzer, Keyence).

Morphological analysis for the EMF parasites degenerated by mAb supplementation, using a transmission electron microscope (TEM)

To analyze the intracellular morphological change of degenerated EMF parasites, TEM observation was performed. EMF parasites were pre-incubated on a six-well culture plate (Sigma-Aldrich Co.) for 24 hs at 27ºC. After the pre-incubation, EMF parasites were incubated in TVM-1 medium containing 15 μg/mL α-rTcEpHbR mAb for 5 days at 27ºC. The parasites were washed three times with PBS, and then fixed by 2% glutalaldehyde in PBS. Prepared samples were analyzed by using TEM in Hanaichi ultrastructure research institute (Aichi, Japan) (137).

Preparation of Hb-depletion TVM-1 medium

GST-rTcEpHbR-affinity beads were prepared by following chapter I. Since commercial FBS used for the parasites culture, which contains 178 μg/mL Hb as certificated by Biowest (Batch No. S10123S1650), the final Hb concentration of 20%

FBS TVM-1 was calculated as 35.6 μg/mL. Excess amount of rTcEpHbR-affinity beads were added into the 20% FBS TVM-1, and then incubated with a shaking at 4ºC for over night, in order to deplete the Hb from medium. The affinity beads were separated from the medium, and kept as the Hb sample that was contained in pre Hb-depletion TVM-1. New rTcEpHbR affinity beads were added into the 300 μl of the medium again, and incubated with a shaking at 4ºC for over night, in order to calculate the residual Hb amount in the post Hb-depletion TVM-1. After the incubation, the rTcEpHbR-affinity beads were removed from the medium again and kept as the Hb sample that was contained in post Hb-depletion TVM-1. The pre and post Hb-depletion sample beads were treated with a SDS-PAGE sample buffer. These samples were spread by SDS-PAGE, and then, stained with Coomassie Brilliant Blue R-250 (CBB) for evaluation of the Hb-depletion efficiency(15). The approximately Hb concentration (*Hb-Con*) in Hb-depletion TVM-1 was estimated by the sample volume (*V*, mL) and CBB staining sensitivity. The detection limit of CBB staining (*S*) is 0.5 μg/cm^2 of protein amount (https://www.thermofisher.com/order/catalog/product/20278). The square measure of one signal band (*A*) was approximated in 0.1 cm^2.

$$Hb\text{-}Con\ (\mu g/ml) < S\ (\mu g/cm^2) * A\ (cm^2)/V$$

Growth-inhibition assay by mAb-1 in Hb-depletion medium

The 1 x 10^5 parasites of EMF were inoculated in each well of a 96-well plate and pre-cultured in for 1 day at 27ºC. Then, the adherent cells were washed with a flesh

TVM-1 to remove the non-adherent cells. One hundred microliters of Hb-depletion medium or 20% FBS TVM-1 which contained 15 μg/ml of mAb-1 or control mAb were added into each well, and then incubated at 27ºC for 5 days. The parasites were morphologically observed by microscopy, and the living cell numbers were evaluated by their BrdU uptake at the time points of 0, 1, 3 and 5 days.

6-3. Results

Preparation of α-rTcEpHbR mAb reactive to living EMF

To assess the possibility of TcEpHbR as a TBV target, α-rTcEpHbR mAb-productive hybridoma cells were prepared. The immunoaffinity of α-rTcEpHbR mAb were evaluated against rTcEpHbR and EMF cell lysate by ELISA and western blotting analysis. In the results of ELISA, 15 lines of hybridoma colonies were selected , in which they produced α-rTcEpHbR-mAb that showed the high O. D. values (> 2.0, data not shown). In the results of western blotting analysis, 13 of the hybridoma cell supernatant, No. 1-3, 5-7, 9-15, exhibited positive reactivities against the EMF crude antigen (Fig. 10). Among them, only mAb No. 10 was reactive against living EMF, which other hybridoma cell supernatants and α-rTcEpHbR mouse immune serum did not react the parasites (Fig. 11). Finally, as the results of IFA, the mAb of No. 10 hybridoma clone that had showed relatively the highest reactivity against living EMF parasites, was selected. The mAb was purified from the supernatant of hybridoma No. 10, and named as mAb-1. The mAb purified from the supernatant of hybridoma No. 9 was used for control mAb. The isotypes of mAb-1 and control mAb were IgG 1 and IgG 2b, respectively (data not shown).

EMF-growth inhibition by supplementation with mAb-1

The growth inhibition activity of α-rTcEpHbR mAb-1 was analyzed. After 5-day incubation with the mAb-1, living numbers of EMF parasite were decreased in a concentration-dependent manner (Fig. 12). In the supplementation of 15 μg/mL and 30

μg/mL α-rTcEpHbR mAb-1, the EMF parasite numbers were significantly reduced to 43% and 18%, as compared to that of the absence of mAb-1 supplementation, respectively ($p < 0.01$, Fig 12A, mAb-1). Furthermore, the EMF cells were swelled under the mAb-1 concentration of 15-30 μg/mL (Fig. 12B, mAb-1). Although the control mAb supplementation in EMF culture also caused a slight cell-proliferation inhibition, it did not cause any morphological changes in the treated EMF (Fig. 12B, control mAb panel).

Epitope mapping by ELISA

To determine epitopes of mAb-1 in TcEpHbR, the epitope mapping analysis were performed by ELISA under the natural (Fig. 13A) and denatured (Fig. 13B) conditions. Anti-TcEpHbR mAb-1 reacted with the 200 and 252 AA of the truncated rTcEpHbRs (fragments H, I and full length, Fig. 13A). In the natural conditions, the optical density (O. D.) values showed over 2.9. On the other hand, other shorter fragments of rTcEpHbR (fragments A-G) did not react with α-rTcEpHbR mAb-1 (O. D. value < 0.035), including the fragment F overlapped a region of fragments H and I. Under the strong denatured conditions of 2, 3, 4 and 6 M of GuHCl, the antigenicities of fragments H and I against mAb-1 were decreased to a half level of natural condition (Fig. 13B). On the other hand, the antigenicities of fragments H and I kept same levels as the natural condition under the concentration of 1 M GuHCl (Fig. 13B).

Interference of α-rTcEpHbR mAb-1 to heme uptake by EMF

The uptake of free-Hb^{A488} in EMF was observed in the presence of α-rTcEpHbR mAb-1 *in vitro*. The EMF-specific uptake of free-Hb^{A488} was visualized as green signals adjacent to the nucleus and kinetoplast, regardless of the presence of mAb-1 (Fig. 14A). The average values of fluorescence intensity each green spot were not significantly differenced between the mAb-1 and control mAb (Fig. 14B).

Morphological analysis of the degenerated EMF parasites

The degenerated EMF parasites that had been co-cultivated with mAb-1 were morphologically analyzed by TEM. EMF parasites were swelled after the incubation with α-rTcEpHbR mAb, fixed by glutalaldehyde and observed by TEM. There were large endocytic vesicles in the both of EMF cells cultured with mAb-1 and control mAb (Fig. 15). However, a large number of electron lucent structures were observed only at cytosol of the degenerated EMF cells cultured with the mAb-1 (Fig. 15, arrow).

EMF-growth inhibition assay by mAb-1 in Hb-depletion condition

Firstly, the results of Hb depletion by a GST pull-down assay were evaluated. Free-Hb occurred as 12.8-kDa α-subunit and 13.0-kDa γ-subunit, as shown in chapter I (Fig. 16A, lanes 1 and 2). After the Hb-depletion treatment, the Hb signals became undetectable level (Fig. 16A, lane 3). The Hb concentration after Hb depletion was estimated under 0.167 μg/mL by the CBB staining sensitivity. Before the Hb depletion, 20% FBS TVM-1 medium contained 34 μg/mL fetal Hb.

The EMF parasites were cultured in the Hb-depleted medium or 20% FBS TVM-1 which contained 15 μg/ml of mAb-1 or control mAb for 5 days, and measured the cell numbers and morphological changes. As the results, after 5-day culture, there was no difference the cell numbers of EMF parasites between in the presence and absence of mAb-1 under the Hb-depletion condition (Fig. 16B, green and orange lines). The growth under Hb depletion was tended to inhibit than under 20% FBS TVM-1 (Fig 16B, red and orange lines). In addition, the remarkable morphological changes were not observed between EMF in the presence and absence of mAb-1 under Hb-depletion, either (Fig. 16C).

6-4. Discussion

The Hb is taken up via TcEpHbR by *T. congolense* EMF as described in chapter I (144). The Hb is considered to be the main heme source in *T. congolense* EMF, because the heme is essential for cell surviving (71, 84, 141). Previously, it was reported that TbHpHbR knockdown in the BSF stage of *T. brucei* caused a growth inhibition in the infected mice (138). In this chapter II, a growth-inhibitory effect of α-rTcEpHbR mAb against the *T. congolense* EMF was examined, in order to evaluate its potential for a TBV.

Firstly, α-rTcEpHbR mAbs were prepared and mAbs that had reacted to EMF cells were selected by ELISA, western blot analysis and IFA. As the results of IFA, α-rTcEpHbR mouse immune serum did not react to the living EMF even though it has reacted to EMF in chapter I. Since fixed cells by methanol change the membrane permeability, the antigenicity of membrane proteins are increased (68). Therefore, α-rTcEpHbR mouse immune serum might react to EMF after fixed by the methanol in chapter I. In other words, the native antigenicity of TcEpHbR might not be high before fixation by the methanol, as the result of the IFA in chapter II. In fact, the 14 clones out of 15 clones of α-rTcEpHbR mAbs did not react against living EMF except mAb-1. These results suggested that the native TcEpHbR was low antigenicity, and mAb-1 was the very scarce antibody which could recognize native TcEpHbR and caused cell degeneration and growth inhibition on EMF.

In the results of epitope mapping analysis, the epitope AAs recognized by mAb-1 were included in the 50-200 AA region, and 1-50 AA region or 200-252 AA regions

was essential as epitope, because the 50-200 AA region (fraction F) had no reactivity against the mAb-1. In addition, truncated rTcEpHbR reactivity against mAb-1 was partially lost under denatured conditions (> 2 M GnHCl, Fig 13B). As high concentration of GnHCl denatured the conformation of antigen, antibodies recognizing three-dimensional structure usually loose the reactivity (55). These findings suggested that the mAb-1 might recognize three-dimensional structure of TcEpHbR. On the other hand, the attenuation of antigenicity was just partial event. The denatured TcEpHbR under relatively lower concentration of GnHCl might refold and regain the antigenicity during washing and/or 1st antibody reaction steps. It suggested that TcEpHbR might have a high refolding ability.

In the results of morphological analysis for the degenerated EMF parasites by TEM, there were a large number of electron lucent vesicles in the cytoplasm of swelling cells treated with mAb-1. In previous study, such electron lucent structures were reported under the knockout of a kinase (eIF2a kinase of *T. cruzi*: TcK2), which involves a regulation of translation factors in *T. cruzi* EMF (5). The TcK2 activated under a condition of heme starvation suppresses the proliferation of *T. cruzi* EMF parasites and promotes the cell differentiation (5). Additionally, the previous study suggested that TcK2 might monitor the levels of intracellular heme presence. Resultantly, the TcK2 knockout caused an increasing of intracellular hydrogen peroxide level, in which the peroxide might damage to *T. cruzi* EMF (5). This previous study suggested that collapse of intracellular heme homeostasis might cause the manifestation of a large number of electron lucent structure with cell proliferation inhibition.

As the results of the interference of mAb-1 to the hemoglobin uptake by EMF, mAb-1 did not inhibit the hemoglobin uptake in EMF. In the result of the growth inhibition assay of EMF using the Hb depleted medium, the growth of EMF under the Hb depletion condition was tended to inhibit compared with TVM-1 medium but the cell swelling of EMF was not observed. Additionally, the effects of cell degeneration and growth inhibition by mAb-1 were completely disappeared under the condition of Hb depletion. These results suggested that the cell degeneration by mAb-1 were caused regardless of Hb depletion and Hb presence was essential for the cell degeneration by mAb-1.

The Hb might be clathrin-mediated endocytosed and transported to a lysosome via early/late endosomes. The endosomes are commonly sorted according to the cargo proteins and transported to appropriate organelle (42, 48, 49). Such transportation systems might be conserved in trypanosomes, because trypanosomes have Rab-family proteins, which involve the membrane trafficking (42, 48, 49). Hb are digested in the lysosome, and heme are released within the lysosome from digested Hb (23). Heme is transported to cytosol via heme transporters that are present at the lysosome membrane, utilized to produce heme proteins (23). The growth inhibition might be caused by Hb/heme shortage inside cell on the EMF parasites that were cultured in Hb-depletion medium. This growth inhibition might be physiologically a normal response because EMF parasites which were infected with tsetse were exposed to hemoglobin depletion during except blood-sucking time of tsetse. Considering the condition of the tsetse proboscis, EMF likely developed a mechanism to adapt themselves to the low

hemoglobin condition. On the other hand, the cell degeneration and growth inhibition might be caused by the interference to the intracellular transportation of Hb in the EMF parasites which were co-cultivated with mAb-1. The electron lucent that were observed in the EMF parasites might be related to the interference. The result of the disappearance of the cell degeneration activity by mAb-1 under Hb depletion condition suggested this hypothesis; TcEpHbR had unknown function involving in Hb/heme transport or metabolism, and mAb-1 inhibited this function. In the result of this inhibition, the intracellular heme homeostasis was disrupted and the heme out of control caused the cell degeneration by its oxidative toxicity.

In this chapter, essential role of Hb was clarified in the EMF proliferation by Hb-depletion assay. My results suggest a potential of TcEpHbR as a target molecule for the development of TBV against *T. congolense* infection.

Table 2. Primers used for epitope mapping analysis

Primer name	Sequence (5'-3')
Epi 1	GGATCC*GCTGAAGGAGAGATCAAGG
Epi 2	GGATCC*AAATCTGAGGAGATCCTCGC
Epi 3	GGATCC*GAGGAAGTTGAAATTGTGGC
Epi 4	GGATCC*TACGTCAAGAAGGCTGCGGA
Epi 5	GCGGCCGC**CTTCACGTGCTCCAATGCAT
Epi 6	GCGGCCGC**CTGGTCCTCGCTTTCTTTCG
Epi 7	GCGGCCGC**GTCCAAAGAGGTCAGAATGG
Epi 8	GCGGCCGC**TGAGGATTCTGTCTCAACCT

Underlines indicate the restriction enzyme sites: **Bam*HI, ***Not*I

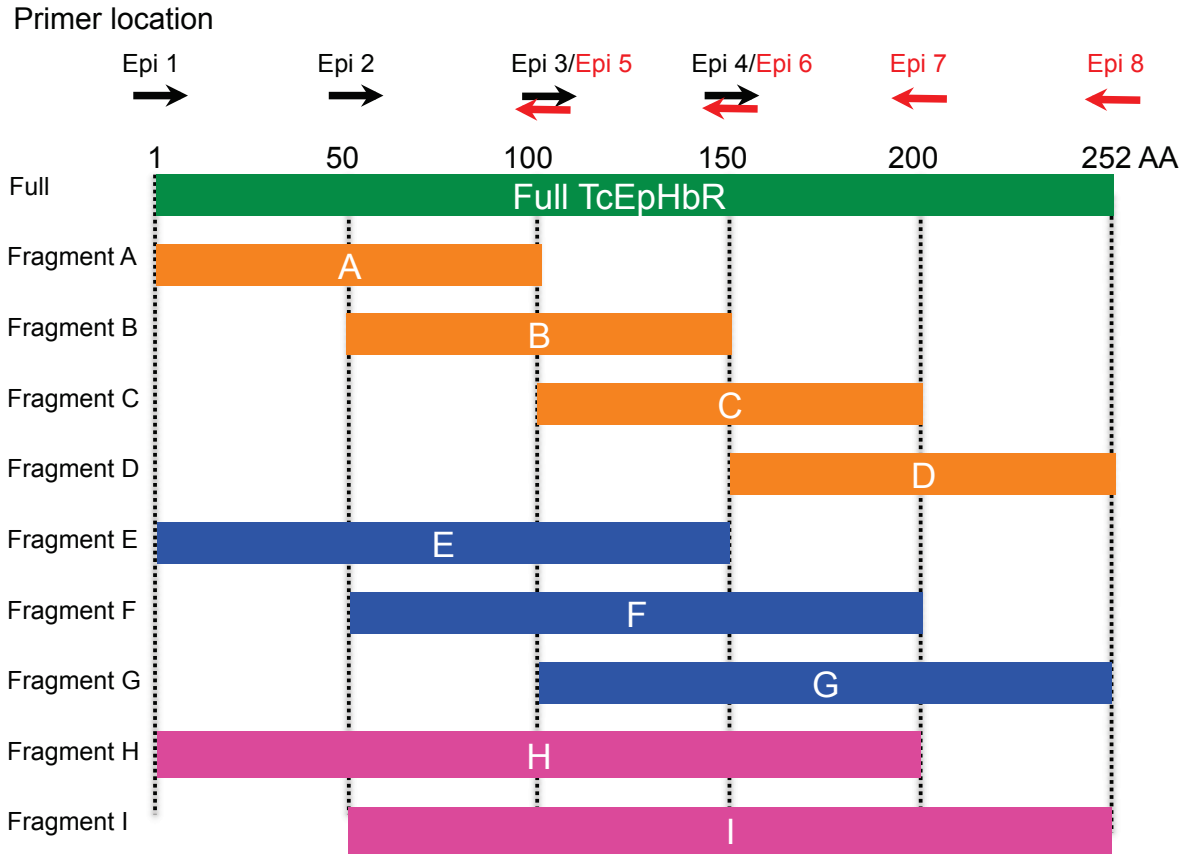

Fig. 9. Truncated rTcEpHbRs. Truncated rTcEpHbR lengths are 100, 150, 200 and 250 AA. The locations of used primers are indicated at upper. Black arrows: forward primers, Red arrows: reverse primers. Each fragment was prepared using each primer set. Full (252 AA, 26.8 kDa): Epi 1/Epi 8, A (102 AA, 10.6 kDa): Epi 1/Epi 5, B (102 AA, 10.6 kDa): Epi 2/Epi6, C(101 AA, 10.7 kDa) : Epi 3/Epi 7, D (99 AA, 10.8 kDa): Epi 4/Epi 8, E (153 AA, 16.0 kDa): Epi 1/Epi 6, F (152 AA, 16.0 kDa): Epi 2/Epi 7, G (150 AA, 16.2 kDa): Epi 3/Epi 8, H (203 AA, 21.3 kDa): Epi 1/ Epi 7, I (201 AA, 21.4 kDa): Epi 2/Epi 8.

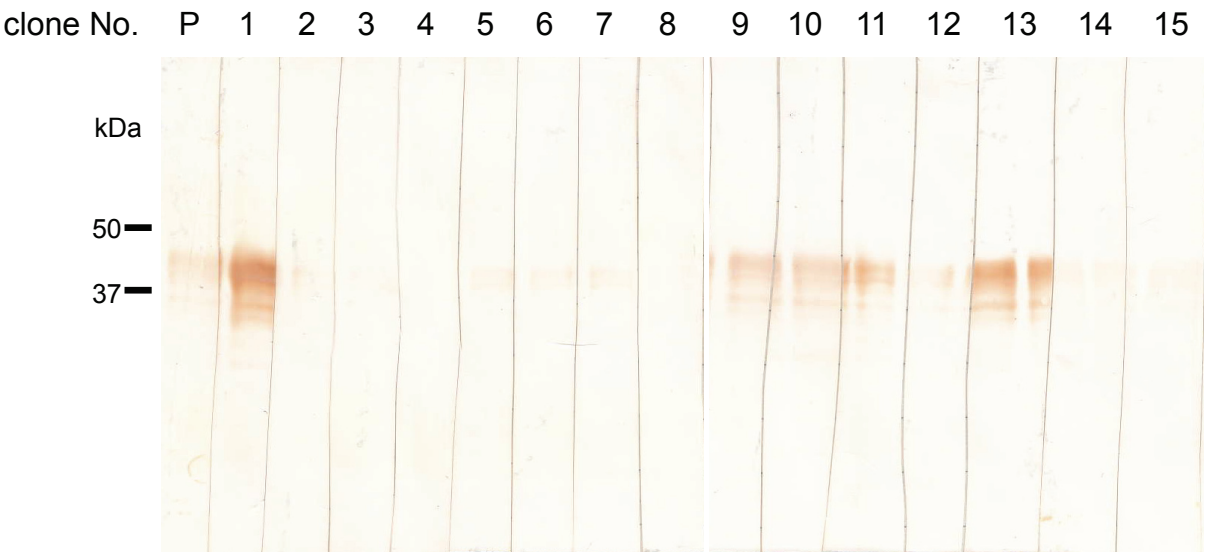

Fig. 10. Evaluation of α-rTcEpHbR mAb activities against *T. congolense* EMF crude antigen. Fifteen lines of hybridoma culture supernatants, which were screened by ELISA, were used as 1st antibody. Total proteins of *T. congolense* EMF were used as antigen. Hybridoma clone numbers are shown at upper. The P indicates positive control (α-rTcEpHbR mouse serum, polyclonal antibody). TcEpHbR signals were shown as two signals, 42 kDa and 37 kDa.

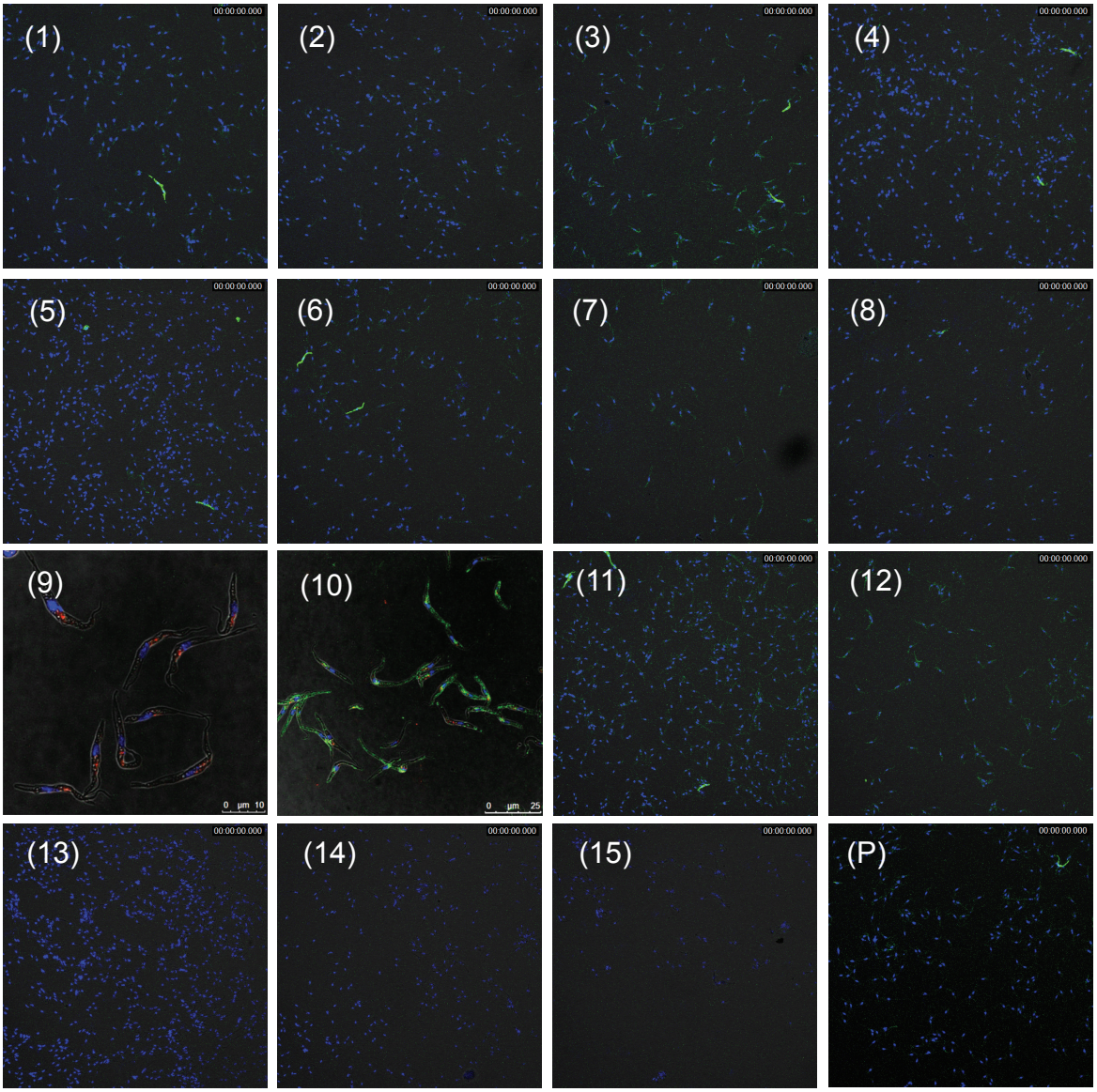

Fig. 11. Reactivities of α-rTcEpHbR antibodies against living EMF by IFA. Alive EMF parasites treated with each hybridoma supernatant or α-rTcEpHbR mouse immune serum were observed by confocal laser scanning microscopy. The antibodies used for IFA are shown at the corner of the panels (clone No. of hybridoma or mouse immune serum (P)). Green signals indicate TcEpHbR. Blue signals indicate nucleus and kinetoplast DNAs and red signals (No. 9, 10) indicate endocytic compartment.

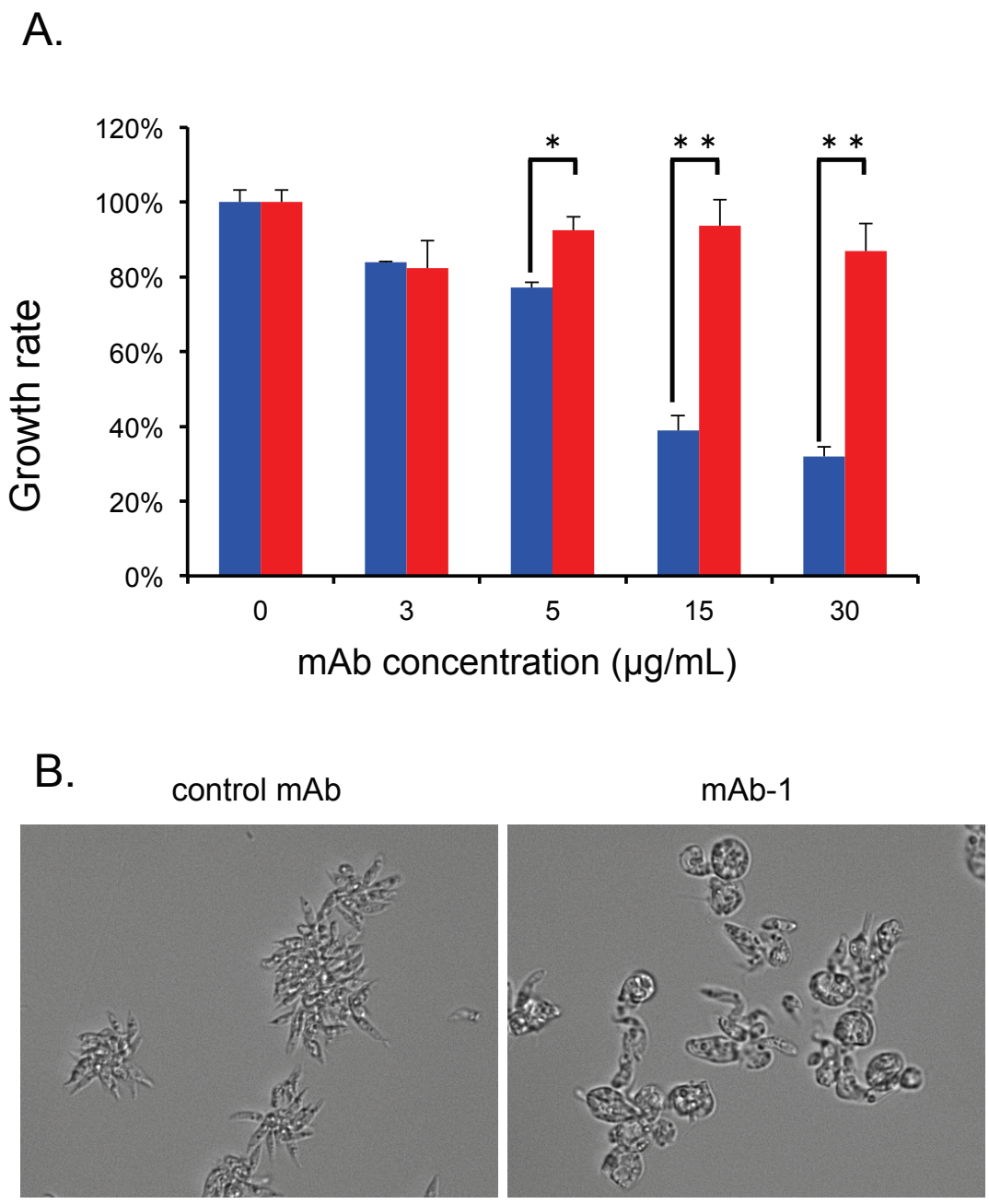

Fig. 12. EMF-growth inhibition assay by mAb-1. A. Cell proliferations were evaluated by BrdU-uptake activity. The data were expressed as the mean chemiluminescence value ± standard deviation. Y-axis: Cell number ratio to negative control (0 μg/mL mAb). Error bar: standard deviation, *: $p < 0.05$, **:$p < 0.01$ **B:** Morphological observation of EMF parasites treated with control mAb and mAb-1. After five-day incubation with 15 μg/mL mAbs, the parasites were observed by light microscopy.

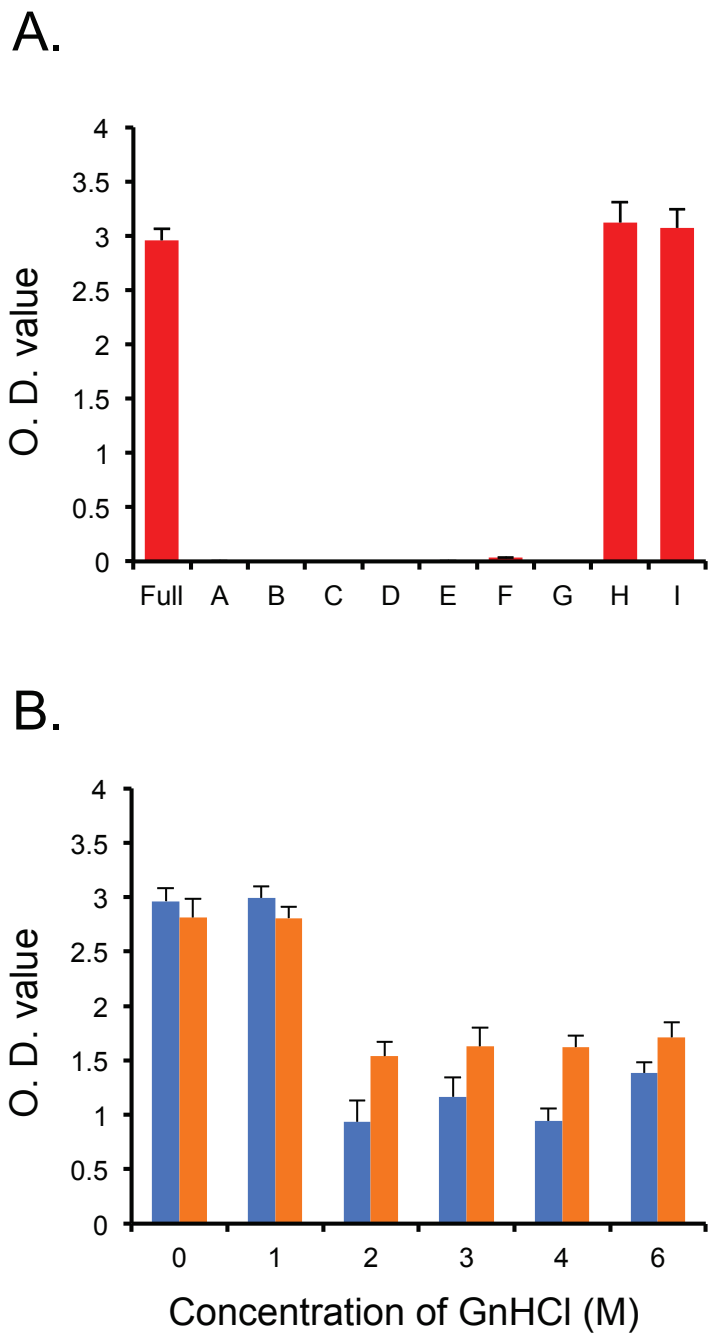

Fig. 13. The epitope mapping analysis against mAb-1 under natural and denatured conditions. A: Under natural condition. The data were expressed as the mean O. D. value ± standard deviation. X-axis indicates the fragments used as antigen. **B:** Under denatured condition. The data were expressed as the mean O. D. value ± standard deviation. X-axis indicates the concentration of GnHCl (M). Blue bar and orange bars indicate ELISA values of fragments H and I, respectively.

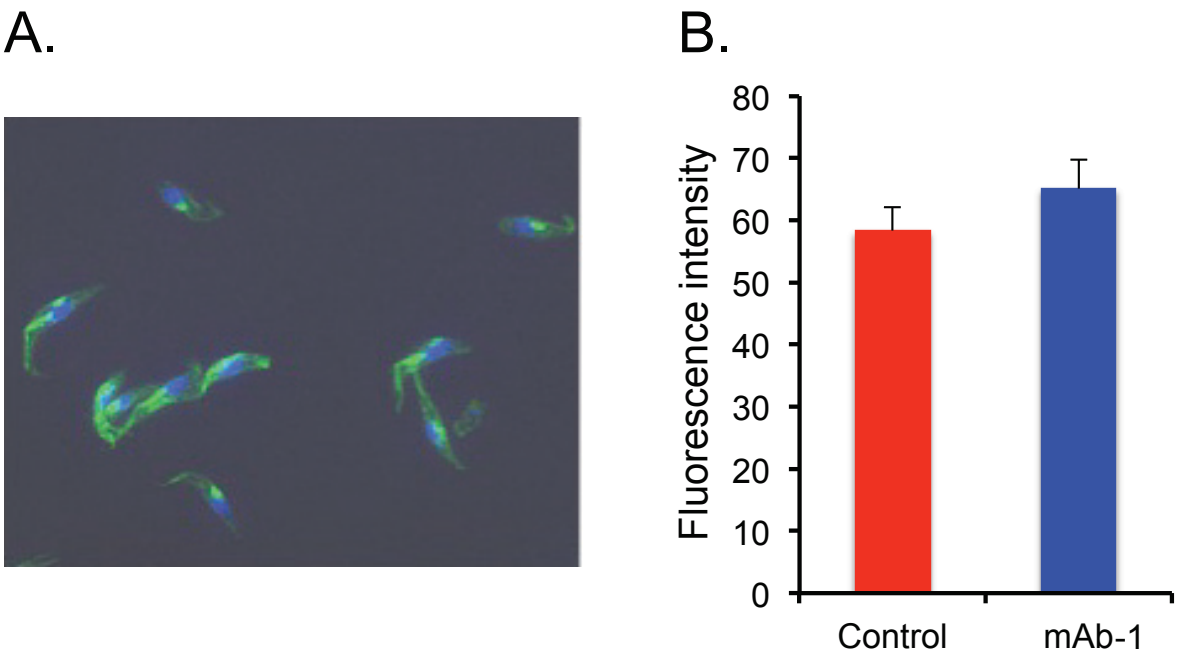

Fig. 14. Interference of α-rTcEpHbR mAb-1 to heme uptake by EMF. A: Fluorescence microscopy of EMF Hb uptake co-cultured with mAb-1. Green: Hb^{A488}, Blue: nucleus and kinetoplast DNAs. **B:** A comparison of fluorescence intensities between the control mAb and mAb-1. The data means fluorescence levels ± standard deviation.

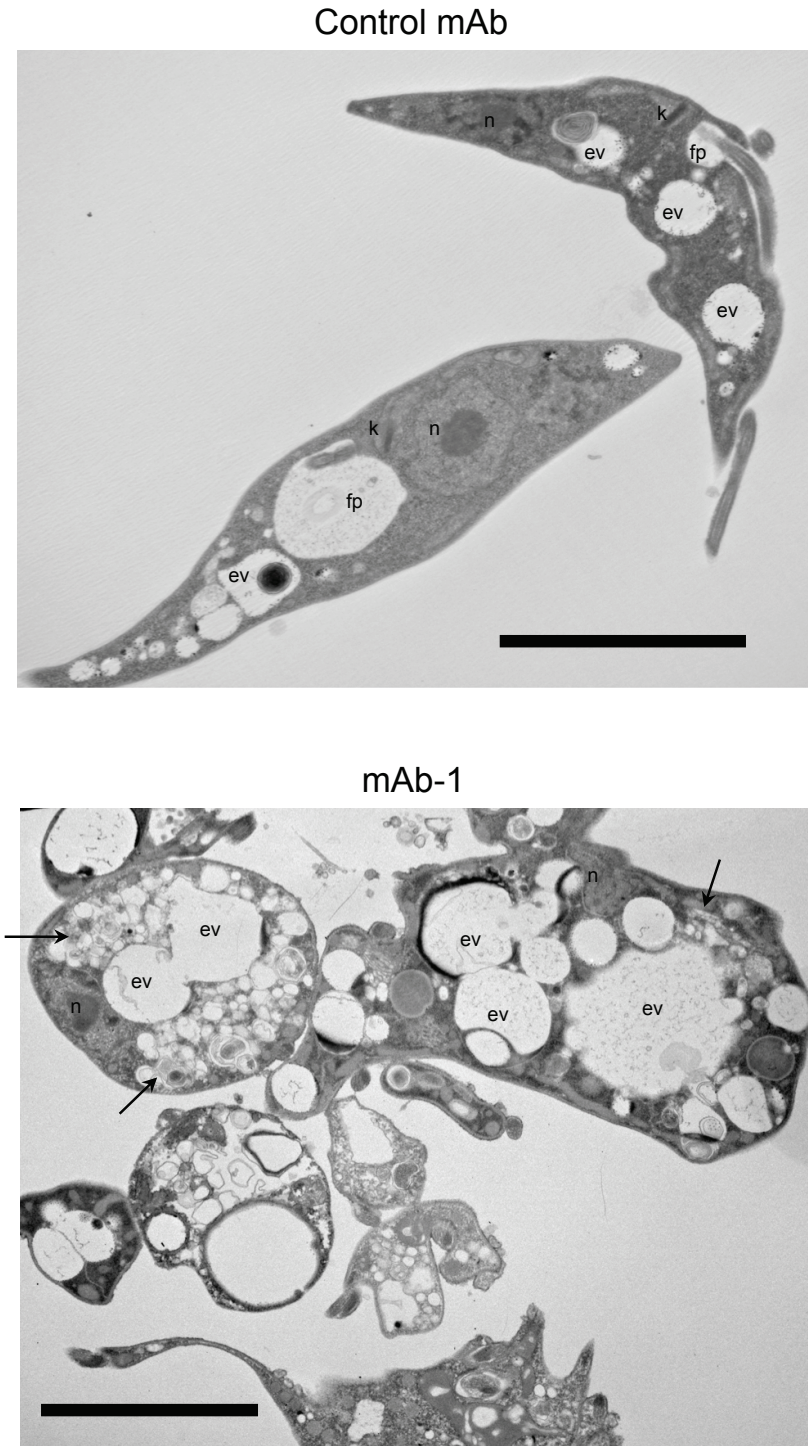

Fig. 15. Morphological analysis of degenerated EMF cells. EMF cells treated with control mAb (upper panel) and with mAb-1 (lower panels) for 5 days. Nucleus (n), kinetoplast (k), flagellar pocket (fp), endocytic vesicle (ev) and electron lucent structure (arrow). Bar = 4 μm

A.

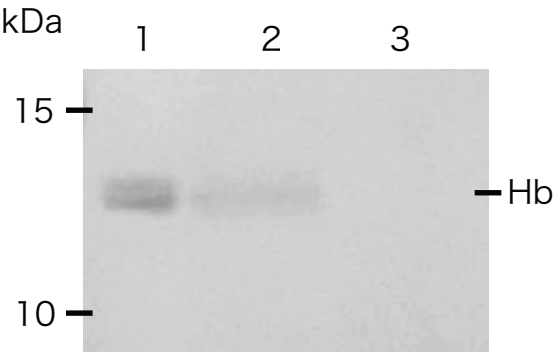

B.

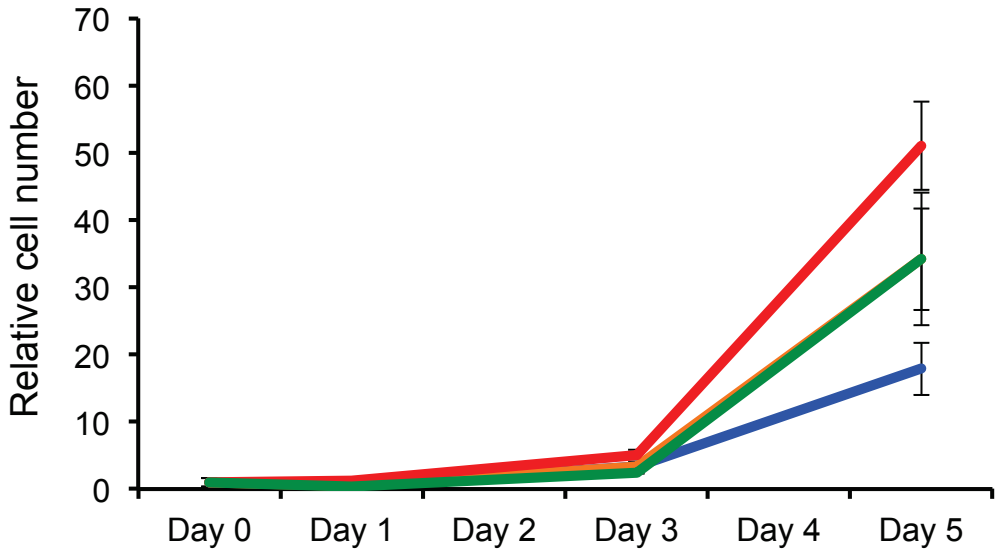

Fig. 14 EMF growth assay in Hb depletion meduim. A: Evaluation of Hb depletion efficiency by SDS-PAGE. The gel was stained with CBB. lane 1: free-Hb indicator, lane 2: before Hb depletion, lane 3: after Hb depletion **B:** EMF growth inhibition assay by mAb-1 in Hb depletion medium. The vertical axis shows the relative cell-number against day 0 (= 1). Red, blue, orange and green lines indicate the cell-number in 20% FBS TVM-1 containing control mAb, in 20% FBS containing mAb-1, in Hb depletion medium containing control mAb and in Hb depletion medium containing mAb-1, respectively.

C.

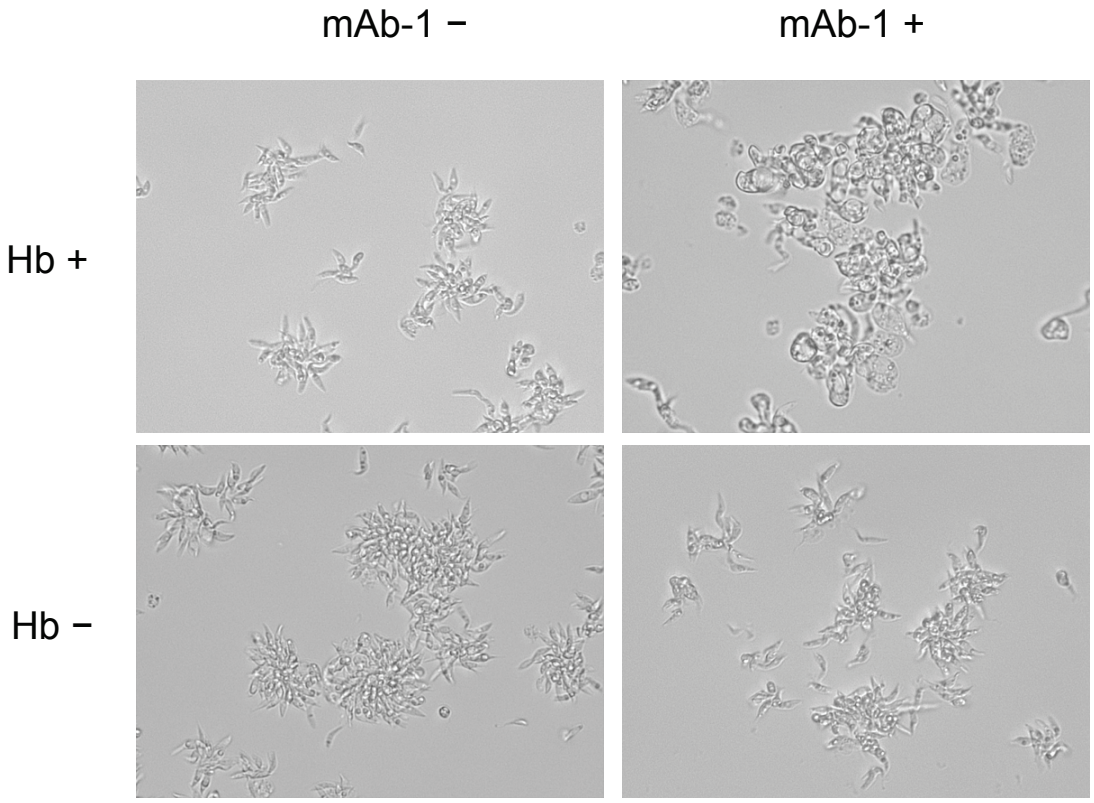

C: Morphological analysis of the EMF cells which were treated with mAb-1under 20% FBS medium (Hb +) and Hb-depletion medium (Hb −) after 5-day cultivation.

7. GENERAL DISCUSSION

Recently, the genome projects for *Trypanosoma brucei brucei, T. b. gambiense, T. congolense* and *T. vivax* were completed (14, 25, 65, 67). The opened genome information combined with cutting-edge molecular biological techniques has contributed extremely to biology of African trypanosomes. In particular, establishment of molecular biological tools for *in vitro* culture systems and manipulation of genome made numerous developments on biological studies of the parasites. However, African trypanosomosis still threatens many people and livestock industry in sub-Saharan Africa (73, 136). Since African trypanosomes can evade from acquired immunity of mammalian host by its antigen variation of VSG in blood circulation, all attempts for vaccine development have been failed until now (56, 74). Because of this difficulty, insect vector stage of trypanosomes have been focused as a new target for trypanosome control (122).

This study aimed to clarify the heme-uptake mechanism of EMF stage, in order to develop a novel trypanosome control strategy in its vector. The *T. congolense* is the only African trypanosome, in which all of the life cycle stages can be maintained *in vitro* (61). Previously, *T. brucei* haptoglobin hemoglobin complex receptor (TbHpHbR) had been reported as the only Hb-uptake receptor identified in African trypanosomes (38, 59, 138). From the results of the whole proteome analysis of *T. congolense*, an orthologue of TbHpHbR was discovered in *T. congolense* (46). Initially, this protein, TcHpHbR, was considered as a HpHb receptor of *T. congolense,* because of its high

similarity to the TbHpHbR (59). However, my study revealed that TcHpHbR considerably differed from TbHpHbR in their expression profiles and ligand specificities. The TbHpHbR was previously reported to be an HpHb-uptake receptor in BSF stage, while I revealed that *T. congolense* exclusively takes up the free-Hb only in EMF stage, indicating the TcHpHbR as a free-Hb uptake receptor in EMF stage. In conclusion of chapter I, therefore TcHpHbR was renamed to *T. congolense* epimastigote-specific free-hemoglobin receptor (TcEpHbR).

Differences between TcEpHbR and TbHpHbR supported the hypothesis that the different ligand specificities of TcEpHbR and TbHpHbR have evolved as a consequence of adaptation of the different life cycle stages of the two species, due to their different habitats within their vector (75). Since *T. congolense* EMF occupy the proboscis of the tsetse fly, they are periodically exposed to a high level of free-Hb during the blood meals of tsetse fly (75). Hence, *T. congolense* EMF may effectively take up the free-Hb by the specific receptor, TcEpHbR. In contrast, *T. brucei* EMF parasitizes the salivary glands of tsetse fly (109). Thus, the parasites do not come in contact with free-Hb. This hypothesis is supported in Lane-Serff *et al.,* 2016 (75). In Lane-Serff *et al.,* 2016, they discuss about the difference of heme-source uptake mechanism between *T. brucei* and *T. congolense* from the evolutionary point of view. Firstly, both of the Hb receptors of *T. congolense* (TcEpHbR) and *T. vivax* (TvHpHbR) were expressed in EMF stage and interacted with free-Hb (66, 144). Secondly, *T. brucei* and *T. congolense* diverged each other after their last common ancestor which had diverged from *T. vivax* (125). From these points of view, TcEpHbR holds more

ancestral property than TbHpHbR, such as binding ability to Hb and expression stage. While TbHpHbR was a modified form for adaption to cellular distribution of *T. brucei*. It was presumed that *T. brucei* EMF firstly have altered their parasitic site from proboscis to salivary grand to evade the toxicity of blood meal or avoid the niche competition with other trypanosome species such as *T. congolense* and *T. vivax*. Because of this alternation of parasitic site, it became difficult to take up Hb from blood meal for *T. brucei* EMF in salivary gland, thus *T. brucei* evolved the new expression pattern and function of its Hb receptor, TbHpHbR, to uptake Hb from mammalian blood in BSF stage. This evolutional view-point can explain the differences of expression stage and function between TbHpHbR and TcEpHbR (75).

In chapter II, the growth-inhibition activity of α-rTcEpHbR mAb against *T. congolense* EMF cells was analyzed to evaluate the possibility of TcEpHbR for a TBV target. An α-rTcEpHbR mAb, named mAb-1, caused cell degeneration and growth inhibition on *T. congolense* EMF. These results suggested that the TcEpHbR might be a target candidate of the TBV. However, the cell degeneration and growth inhibition mechanisms have not been elucidated yet fully.

The EMF cell degeneration and growth inhibition in the presence of mAb-1 was not caused by an inhibition of the Hb uptake by TcEpHbR. On the other hand, the EMF growth was decreased in the presence of mAb-1 and Hb depletion condition. Additionally, the electron lucent vesicles were appeared in the swelling EMF cells. Because electron lucent vesicles were previously reported as the result of intracellular heme starvation, the lucent vesicles observed in this study might be the result of heme

starvation (5). As a hypothesis from these results and studies, mAb-1 might interfere the normal intracellular transport and/or metabolism of Hb by unknown mechanisms. It might cause a collapse of intracellular heme homeostasis, and then, the cell degeneration and growth inhibition of EMF would be led.

The study showed that TcEpHbR was a novel receptor to take up heme source from the blood sucked by tsetse fly to *T. congolense.* In addition, I revealed the different function and expression profiles between TcEpHbR and TbHpHbR. This difference may occur from evolutional transition of parasitic site of *T. congolense* and *T. brucei* in tsetse fly (75). Furthermore, the potential of TcEpHbR was presented for a TBV target, in which one α-rTcEpHbR mAb (mAb-1) caused cell degeneration and growth inhibition of *T. congolese* EMF *in vitro*. On the other hand, the low antigenicity of TcEpHbR will act as a barrier to develop the TBV. As a possibility, the peptide vaccine which targets the epitope of mAb-1 will be able to resolve this problem. Alternatively, the unknown mechanism of effect of mAb-1 may be involved in other candidates for TBVs or drugs. As a future plan, it needs to be elucidated that detail mechanisms of effects of mAb-1, for the development of novel TBV, as well as for clarifying the basic biology of trypanosomes.

8. CONCLUSSION

This thesis mainly reported the identification, molecular characterization and evaluation as a novel target for transmission blocking vaccine (TBV) of *Trypanosoma congolense* epimastigote-specific free-hemoglobin receptor (TcEpHbR).

In order to identify heme-uptake receptor in *T. congolense*, a *T. brucei* haptoglobin hemoglobin complex receptor (TbHpHbR) orthologue (*T. congolense* haptoglobin hemoglobin complex receptor, TcHpHbR) was sought from whole genome and proteome databases. The results of the gene- and protein-expression profiles of TcHpHbR revealed that TcHpHbR was exclusively expressed in the epimastigote form (EMF) of parasite, and localized at both EMF cell surface and flagellar pocket. Furthermore, the results of molecular-interaction analyses between TcHpHbR and free-Hb, free-Hp or HpHb, clarified that the TcHpHbR had a high affinity with free-Hb. Additionally, in the analysis of Hb uptake in all the life-cycle stages of *T. congolense, T. congolense* was shown to only take up free-Hb in EMF stage, but not to take up other hemoglobin associated proteins, free-Hp and HpHb complex, in other life-cycle stages. These results indicated that TcHpHbR functioned as the free-Hb receptor in EMF stage of *T. congolense.* Therefore, renamed the TcHpHbR was renamed to *T. congolense* epimastigote-specific free-hemoglobin receptor, TcEpHbR (Chapter I).

Next, the potential of TcEpHbR was examined for the development of TBV. Firstly, the α-rTcEpHbR monoclonal antibody (mAb), which reacted with living EMF of *T. congolense,* was prepared. The prepared mAb, mAb-1, caused cell degeneration

toward the parasites and induced growth inhibition on the EMF of parasites. However, the detailed mechanisms of cell degeneration and growth inhibition were not clarified. Results of morphological analyses and EMF-growth inhibition assay in the Hb-depletion condition suggested a possibility that TcEpHbR might participate in intracellular Hb transportation and/or intracellular heme homeostasis of the parasites. The findings of this study suggested that TcEpHbR could become a candidate for TBV target to control AAT (Chapter II).

Here, it was revealed that TcEpHbR was a novel Hb receptor of *T. congolense* EMF stage and that the antibody against TcEpHbR could inhibit a proliferation of *T. congolense* EMF *in vitro*. The mechanisms of EMF cell degeneration and growth inhibition should be clarified in future.

9. ACKNOWLEDGEMENTS

This research work was carried out at the National Research Center for Protozoan Diseases (NRCPD), Obihiro University of Agriculture and Veterinary Medicine. This research was financially supported by Sasagawa-Foundation and the Young Researcher Development Program from Gifu University.

I owe my cordial gratitude to my supervisor Prof. Naoaki Yokoyama (NRCPD) for intellectual guidance, constructive criticism and encouragement during the period of this study. I express my deepest gratitude to Prof. Noboru Inoue (Executive vice president, Director, Obihiro University of Agriculture and Veterinary Medicine) for his perennial supervision, spirit of forbearance and teaching me profundity of parasitology. I am deeply grateful to Assoc. Prof. Shinya Fukumoto (NRCPD) for his insightful comments and suggestions. I owe a very important debt to Project Assistant Prof. Keisuke Suganuma (Research Center for Global Agromedicine) for his constructive comments, warm encouragement and enormous help to me.

I wish express my gratitude to Prof. Shin-ichiro Kawazu (NRCPD), Tadashi Itagaki (Iwate University), Assoc. Prof. Tetsuya Furuya (Tokyo University of Agriculture and Technology) and Assoc. Prof. Yasuhiro Takashima (Gifu University) for their valuable suggestion and their patience in revising this dissertation.

I am deeply grateful to Prof. Xuenan Xuan, Prof. Ikuo Igarashi, Prof. Hiroshi Suzuki, Prof. Makoto Igarashi, Assoc. Prof. Kentaro Kato, Assoc. Prof. Yoshifumi

Nishikawa and Assistant. Prof. Rika Umemiya-Shirafuji for their critical reviews for my progress report during the NRCPD seminar.

I am greatly appreciative of former and current members of the Research Unit for Advanced Preventive Medicine and Research Unit for Vector Biology. And I am deeply grateful to the all of former and current NRCPD researchers, officers, secretaries, technical assistants and students.

I also thank Assoc. Prof. Junya Yamagishi, Dr. Tadashi Okada, Assistant Prof. Masahito Asada, Assistant Prof. Tatsunori Masatani, Assistant Prof. Madoka Ichikawa-Seki and Ms. Wakako Furuyama to support my fun academic life.

Lastly, I thank greatly my parents Takafumi Yamasaki and Yumi Yamasaki, my elder brother Kohei Yamasaki for everlasting love of family. I am eternally grateful to my grandparents Teruo Yamasaki, Reiko Yamasaki, Yoshiaki Katano and Sayoko Katano for giving me the original experiments that aspire the way of my research. I thank my beloved cats, Tetra and Qui, for their selfless healing also. And I grateful thank my fiancé Dr. Tatsuki Sugi for supporting and cheering up me every time.

10. REFRENCES

1. Acosta-Serrano, A., Vassella, E., Liniger, M., Kunz Renggli, C., Brun, R., Roditi, I., Englund, P. T. (2001). The surface coat of procyclic *Trypanosoma brucei:* programmed expression and proteolytic cleavage of procyclin in the tsetse fly. PNAS. 98, 1513~1518.
2. Agarwal, S., Rastogi, R., Gupta, D., Patel, N., Raje, M., Mukhopadhyay, A. (2013). Clathrin-mediated hemoglobin endocytosis is essential for survival of *Leishmania*. BBA-Molecular Cell Research. 1833, 1065~1077.
3. Aksoy, S. (2003). Control of tsetse flies and trypanosomes using molecular genetics. Vet Parasitol. 115, 125~145.
4. Anene, B. M., Onah, D. N., Nawa, Y. (2001). Drug resistance in pathogenic African trypanosomes: what hopes for the future? Vet Parasitol. 96, 83-100.
5. Augusto, L. D., Moretti, N. S., Ramos, T. C. P., de Jesus, T. C. L., Zhang, M., Castilho, B. A., Schenkman, S. (2015). A Membrane-bound eIF2 Alpha Kinase Located in Endosomes Is Regulated by Heme and Controls Differentiation and ROS Levels in *Trypanosoma cruzi*. PLOS Pathog. 11, e1004618.
6. Auty, H., Anderson, N. E., Picozzi, K., Lembo, T., Mubanga, J., Hoare, R., Fyumagwa, R. D., Mable, B., Hamill, L., Cleaveland, S., Welburn, S. C. (2012). Trypanosome diversity in wildlife species from the serengeti and Luangwa Valley ecosystems. PLoS Negl Trop Dis. 6, e1828.
7. Babin, D. R., Schroeder, W. A., Shelton, J. R., Shelton, J. B., Robberson, B.

(1966). The amino acid sequence of the gamma chain of bovine fetal hemoglobin. Biochemistry. 5, 1297~1310.

8. Babokhov, P., Sanyaolu, A. O., Oyibo, W. A., Fagbenro-Beyioku, A. F., Iriemenam, N. C. (2013). A current analysis of chemotherapy strategies for the treatment of human African trypanosomiasis. Pathog Glob Health. 107, 242~252.

9. Banci, L. (1997). Structural properties of peroxidases. J Biotechnol. 53, 253~263.

10. Barupala, D. P., Dzul, S. P., Riggs-Gelasco, P. J., Stemmler, T. L. (2016). Synthesis, delivery and regulation of eukaryotic heme and Fe-S cluster cofactors. Arch Biochem Biophys. 592, 60-75.

11. Batlle A. M. del C., Ferramola, A. M., Grinstein, M. (1967). Purification and general properties of sigma-aminolaevulate dehydratase from cow liver. Biochem J. 104, 6.

12. Bazzocco, S., Dopeso, H., Carton-Garcia, F., Macaya, I., Andretta, E., Chionh, F., Rodrigues, P., Garrido, M., Alazzouzi, H., Nieto, R., Sanchez, A., Schwartz, S., Jr., Bilic, J., Mariadason, J. M., Arango, D. (2015). Highly Expressed Genes in Rapidly Proliferating Tumor Cells as New Targets for Colorectal Cancer Treatment. Clin Cancer Res. 21, 3695~3704.

13. Beecroft, R. P., Roditi, I., Pearson, T. W. (1993). Identification and characterization of an acidic major surface glycoprotein from procyclic stage *Trypanosoma congolense*. Mol Biochem Parasitol. 61, 285-294.

14. Berriman, M., Ghedin, E., Hertz-Fowler, C., Blandin, G., Renauld, H., Bartholomeu, D. C., Lennard, N. J., Caler, E., Hamlin, N. E., Haas, B. (2005). The genome of the African trypanosome *Trypanosoma brucei*. Science. 309, 416~422.

15. Bhattacharya, D., Mukhopadhyay, D., Chakrabarti, A. (2007). Hemoglobin depletion from red blood cell cytosol reveals new proteins in 2-D gel-based proteomics study. Proteomics Clin Appl. 1, 561~564.

16. Bhattacharyya, A., Chattopadhyay, R., Mitra, S., Crowe, S. E. (2014). Oxidative stress: an essential factor in the pathogenesis of gastrointestinal mucosal diseases. Physiol Rev. 94, 329~354.

17. Bienen, E., Webster, P., Fish, W. (1991). *Trypanosoma* (Nannomonas) *congolense*:Changes in respiratory metabolism during the life cycle. Exp Parasitol. 73, 403~412.

18. Bringaud, F., Riviere, L., Coustou, V. (2006). Energy metabolism of trypanosomatids: adaptation to available carbon sources. Mol Biochem Parasitol. 149, 1~9.

19. Brun, R. (1982). Cultivation of procyclic trypomastigotes of *Trypanosoma congolense* in a semi-defined medium with direct adaptation from bloodstream forms. Z Parasitenkd. 67, 129~135.

20. Brun, R., Blum, J., Chappuis, F., Burri, C. (2010). Human African trypanosomiasis. Lancet. 375, 148-159.

21. Buehler, P. W., D'Agnillo, F. (2010). Toxicological consequences of

extracellular hemoglobin: biochemical and physiological perspectives. Antioxid Redox Signal. 12, 275~291.

22. Bull, C. G., Bartual, L. (1920). Pneumococcus Cultures in Whole Fresh Blood : I. The Retardative Effect of the Blood of Immune Animals and the Mechanism of the Phenomenon. J Exp Med. 31, 233~251.

23. Cabello-Donayre, M., Malagarie-Cazenave, S., Campos-Salinas, J., Galvez, F. J., Rodriguez-Martinez, A., Pineda-Molina, E., Orrego, L. M., Martinez-Garcia, M., Sanchez-Canete, M. P., Estevez, A. M., Perez-Victoria, J. M. (2016). Trypanosomatid parasites rescue heme from endocytosed hemoglobin through lysosomal HRG transporters. Mol Microbiol. 101, 895~908.

24. Campos-Salinas, J., Cabello-Donayre, M., Garcia-Hernandez, R., Perez-Victoria, I., Castanys, S., Gamarro, F., Perez-Victoria, J. M. (2011). A new ATP-binding cassette protein is involved in intracellular haem trafficking in *Leishmania*. Mol Microbiol. 79, 1430-1444.

25. Carnes, J., Anupama, A., Balmer, O., Jackson, A., Lewis, M., Brown, R., Cestari, I., Desquesnes, M., Gendrin, C., Hertz-Fowler, C., Imamura, H., Ivens, A., Koreny, L., Lai, D. H., MacLeod, A., McDermott, S. M., Merritt, C., Monnerat, S., Moon, W., Myler, P., Phan, I., Ramasamy, G., Sivam, D., Lun, Z. R., Lukes, J., Stuart, K., Schnaufer, A. (2015). Genome and phylogenetic analyses of *Trypanosoma evansi* reveal extensive similarity to *T. brucei* and multiple independent origins for dyskinetoplasty. PLoS Negl Trop Dis. 9, e3404.

26. Cenci, U., Moog, D., Curtis, B. A., Tanifuji, G., Eme, L., Lukes, J., Archibald, J.

M. (2016). Heme pathway evolution in kinetoplastid protists. BMC Evol Biol. 16, 109.

27. Chang, Y. T., Stiffelman, O. B., Loew, G. H. (1996). Computer modeling of 3D structures of cytochrome P450s. Biochimie. 78, 771~779.

28. Chappuis, F., Pittet, A., Bovier, P. A., Adams, K., Godineau, V., Hwang, S. Y., Magnus, E., Buscher, P. (2002). Field evaluation of the CATT/*Trypanosoma brucei gambiense* on blood-impregnated filter papers for diagnosis of human African trypanosomiasis in southern Sudan. Trop Med Int Health. 7, 942~948.

29. Coates, C. J., Decker, H. (2016). Immunological properties of oxygen-transport proteins: hemoglobin, hemocyanin and hemerythrin. Cell Mol Life Sci.

30. Coustou, V., Guegan, F., Plazolles, N., Baltz, T. (2010). Complete in vitro life cycle of *Trypanosoma congolense*: development of genetic tools. PLoS Negl Trop Dis. 4, e618.

31. Coutinho-Abreu, I. V., Ramalho-Ortigao, M. (2010). Transmission blocking vaccines to control insect-borne diseases: a review. Mem Inst Oswaldo Cruz. 105, 1~12.

32. Coutinho-Abreu, I. V., Sharma, N. K., Robles-Murguia, M., Ramalho-Ortigao, M. (2010). Targeting the midgut secreted PpChit1 reduces *Leishmania major* development in its natural vector, the sand fly Phlebotomus papatasi. PLoS Negl Trop Dis. 4, e901.

33. Cupello, M. P., Souza, C. F. d., Buchensky, C., Soares, J. B. R. C., Laranja, G. A. T., Coelho, M. G. P., Cricco, J. A., Paes, M. C. (2011). The heme uptake

process in *Trypanosoma cruzi* epimastigotes is inhibited by heme analogues and by inhibitors of ABC transporters. Acta Tropica. 120, 211~218.

34. Dai, J., Wang, P., Adusumilli, S., Booth, C. J., Narasimhan, S., Anguita, J., Fikrig, E. (2009). Antibodies against a tick protein, Salp15, protect mice from the Lyme disease agent. Cell Host Microbe. 6, 482-492.

35. Davis, J. M., Pennington, J. E., Kubler, A. M., Conscience, J. F. (1982). A simple, single-step technique for selecting and cloning hybridomas for the production of monoclonal antibodies. J Immunol Methods. 50, 161~171.

36. de Verdier, C. H., Garby, L. (1969). Low binding of 2,3-diphosphoglycerate to haemoglobin F. A contribution to the knowledge of the binding site and an explanation for the high oxygen affinity of foetal blood. Scand J Clin Lab Invest. 23, 149~151.

37. Deisseroth, A., Dounce, A. L. (1970). Catalase: Physical and chemical properties, mechanism of catalysis, and physiological role. Physiol Rev. 50, 319~375.

38. DeJesus, E., Kieft, R., Albright, B., Stephens, N. A., Hajduk, S. L. (2013). A single amino acid substitution in the group 1 *Trypanosoma brucei gambiense* haptoglobin-hemoglobin receptor abolishes TLF-1 binding. PLoS Pathog. 9, e1003317.

39. Delves, M. J., Ramakrishnan, C., Blagborough, A. M., Leroy, D., Wells, T. N., Sinden, R. E. (2012). A high-throughput assay for the identification of malarial transmission-blocking drugs and vaccines. Int J Parasitol. 42, 999~1006.

40. Desquesnes, M., Davila, A. M. (2002). Applications of PCR-based tools for detection and identification of animal trypanosomes: a review and perspectives. Vet Parasitol. 109, 213~231.

41. Deuel, J. W., Schaer, C. A., Boretti, F. S., Opitz, L., Garcia-Rubio, I., Baek, J. H., Spahn, D. R., Buehler, P. W., Schaer, D. J. (2016). Hemoglobinuria-related acute kidney injury is driven by intrarenal oxidative reactions triggering a heme toxicity response. Cell Death Dis. 7, e2064.

42. Dhir, V., Goulding, D., Field, M. C. (2004). TbRAB1 and TbRAB2 mediate trafficking through the early secretory pathway of *Trypanosoma brucei*. Mol Biochem Parasitol. 137, 253~265.

43. Djohan, V., Kaba, D., Rayaisse, J. B., Dayo, G. K., Coulibaly, B., Salou, E., Dofini, F., Kouadio Ade, M., Menan, H., Solano, P. (2015). Detection and identification of pathogenic trypanosome species in tsetse flies along the Comoe River in Cote d'Ivoire. Parasite. 22, 18.

44. Engstler, M., Thilo, L., Weise, F., Grunfelder, C. G., Schwarz, H., Boshart, M., Overath, P. (2004). Kinetics of endocytosis and recycling of the GPI-anchored variant surface glycoprotein in *Trypanosoma brucei*. J Cell Sci. 117, 1105~1115.

45. Evans, D. A., Ellis, D. S., Stamford, S. (1979). Ultrastructural studies of certain aspects of the development of *Trypanosoma congolense* in *Glossina morsitans morsitans*. J Protozool. 26, 557~563.

46. Eyford, B. A., Sakurai, T., Smith, D., Loveless, B., Hertz-Fowler, C., Donelson,

J. E., Inoue, N., Pearson, T. W. (2011). Differential protein expression throughout the life cycle of *Trypanosoma congolense*, a major parasite of cattle in Africa. Mol Biochem Parasitol. 177, 116~125.

47. Fenn, K., Matthews, K. R. (2007). The cell biology of *Trypanosoma brucei* differentiation. Curr Opin Microbiol. 10, 539-546.

48. Field, H., Farjah, M., Pal, A., Gull, K., Field, M. C. (1998). Complexity of trypanosomatid endocytosis pathways revealed by Rab4 and Rab5 isoforms in *Trypanosoma brucei*. J Biol Chem. 273, 32102~32110.

49. Field, M. C., Boothroyd, J. C. (1995). *Trypanosoma brucei:* molecular cloning of homologues of small GTP-binding proteins involved in vesicle trafficking. Exp Parasitol. 81, 313~320.

50. Field, M. C., Carrington, M. (2009). The trypanosome flagellar pocket. Nat Rev Microbiol. 7, 775~786.

51. Fish, W. R., Muriuki, C. W., Muthiani, A. M., Grab, D. J., Lonsdale-Eccles, J. D. (1989). Disulfide bond involvement in the maintenance of the cryptic nature of the cross-reacting determinant of metacyclic forms of *Trypanosoma congolense*. Biochemistry. 28, 5415~5421.

52. Franco, J. R., Simarro, P. P., Diarra, A., Jannin, J. G. (2014). Epidemiology of human African trypanosomiasis. Clin Epidemiol. 6, 257~275.

53. Frydman, B., Frydman, R. B., Valasinas, A., Levy, E. S., Feinstein, G. (1976). Biosynthesis of uroporphyrinogens from porphobilinogen: mechanism and the nature of the process. Philos Trans R Soc Lond B Biol Sci. 273, 137-160.

54. Gkoumassi, E., Dijkstra-Tiekstra, M. J., Hoentjen, D., de Wildt-Eggen, J. (2012). Hemolysis of red blood cells during processing and storage. Transfusion. 52, 489~492.

55. Grathwohl, K. U., Horiuchi, M., Ishiguro, N., Shinagawa, M. (1997). Sensitive enzyme-linked immunosorbent assay for detection of PrP(Sc) in crude tissue extracts from scrapie-affected mice. J Virol Methods. 64, 205-216.

56. Guengerich, F. P. (2008). Cytochrome p450 and chemical toxicology. Chem Res Toxicol. 21, 70~83.

57. Haberer, J. E., Musiimenta, A., Atukunda, E. C., Musinguzi, N., Wyatt, M. A., Ware, N. C., Bangsberg, D. R. (2016). Short message service (SMS) reminders and real-time adherence monitoring improve antiretroviral therapy adherence in rural Uganda. AIDS. 30, 1295~1300.

58. Hibbard, E. D. (1972). Folate and vitamin B12 metabolism in pregnancy. Midwife Health Visit. 8, 280~282.

59. Higgins, M. K., Tkachenko, O., Brown, A., Reed, J., Raper, J., Carrington, M. (2013). Structure of the trypanosome haptoglobin–hemoglobin receptor and implications for nutrient uptake and innate immunity. Proc Natl Acad Sci. 110, 1905~1910.

60. Hirumi, H., Hirumi, K. (1989). Continuous cultivation of *Trypanosoma brucei* blood stream forms in a medium containing a low concentration of serum protein without feeder cell layers. J Parasitol. 75, 985~989.

61. Hirumi, H., Hirumi, K. (1991). In vitro cultivation of *Trypanosoma congolense*

bloodstream forms in the absence of feeder cell layers. Parasitology. 102, 225~236.

62. Hsu, W. P., Miller, G. W. (1970). Coproporphyrinogenase in tobacco (*Nicotiana tabacum L.*). Biochem J. 117, 215~220.

63. Huynh, C., Yuan, X., Miguel, D. C., Renberg, R. L., Protchenko, O., Philpott, C. C., Hamza, I., Andrews, N. W. (2012). Heme uptake by *Leishmania amazonensis* is mediated by the transmembrane protein LHR1. PLoS Pathog. 8, e1002795.

64. Jackson, A. H., Sancovich, H. A., Ferramola, A. M., Evans, N., Games, D. E., Matlin, S. A., Elder, G. H., Smith, S. G. (1976). Macrocyclic intermediates in the biosynthesis of porphyrins. Philos Trans R Soc Lond B Biol Sci. 273, 191~206.

65. Jackson, A. P., Berry, A., Aslett, M., Allison, H. C., Burton, P., Vavrova-Anderson, J., Brown, R., Browne, H., Corton, N., Hauser, H., Gamble, J., Gilderthorp, R., Marcello, L., McQuillan, J., Otto, T. D., Quail, M. A., Sanders, M. J., van Tonder, A., Ginger, M. L., Field, M. C., Barry, J. D., Hertz-Fowler, C., Berriman, M. (2012). Antigenic diversity is generated by distinct evolutionary mechanisms in African trypanosome species. Proc Natl Acad Sci U S A. 109, 3416-3421.

66. Jackson, A. P., Goyard, S., Xia, D., Foth, B. J., Sanders, M., Wastling, J. M., Minoprio, P., Berriman, M. (2015). Global gene expression profiling through the complete life cycle of *Trypanosoma vivax*. PLoS Negl Trop Dis. 9, e0003975.

67. Jackson, A. P., Sanders, M., Berry, A., McQuillan, J., Aslett, M. A., Quail, M. A., Chukualim, B., Capewell, P., MacLeod, A., Melville, S. E., Gibson, W., Barry, J. D., Berriman, M., Hertz-Fowler, C. (2010). The genome sequence of *Trypanosoma brucei gambiense*, causative agent of chronic human african trypanosomiasis. PLoS Negl Trop Dis. 4, e658.

68. Jiang, H. P., Serrero, G. (1992). Isolation and characterization of a full-length cDNA coding for an adipose differentiation-related protein. PNAS. 89, 7856~7860.

69. Kennedy, P. G. (2006). Diagnostic and neuropathogenesis issues in human African trypanosomiasis. Int J Parasitol. 36, 505~512.

70. Kennedy, P. G. (2013). Clinical features, diagnosis, and treatment of human African trypanosomiasis (sleeping sickness). Lancet Neurol. 12, 186~194.

71. Khan, A. A., Quigley, J. G. (2011). Control of intracellular heme levels: heme transporters and heme oxygenases. Biochim Biophys Acta. 1813, 668~682.

72. Kristiansen, M., Graversen, J. H., Jacobsen, C., Sonne, O., Hoffman, H. J., Law, S. K., Moestrup, S. K. (2001). Identification of the haemoglobin scavenger receptor. Nature. 409, 198~201.

73. Kristjanson, P., Swallow, B. M., Rowlands, G., Kruska, R., De Leeuw, P. (1999). Measuring the costs of African animal trypanosomosis, the potential benefits of control and returns to research. Agric Syst. 59, 79~98.

74. La Greca, F., Magez, S. (2011). Vaccination against trypanosomiasis: can it be done or is the trypanosome truly the ultimate immune destroyer and escape

artist? Hum Vaccin. 7, 1225~1233.

75. Lane-Serff, H., MacGregor, P., Peacock, L., Macleod, O. J., Kay, C., Gibson, W., Higgins, M. K., Carrington, M. (2016). Evolutionary diversification of the trypanosome haptoglobin-haemoglobin receptor from an ancestral haemoglobin receptor. Elife. 5, e13044.

76. Lanham, S. M., Godfrey, D. (1970). Isolation of salivarian trypanosomes from man and other mammals using DEAE-cellulose. Exp Parasitol. 28, 521~534.

77. Lara, F., Sant'Anna, C., Lemos, D., Laranja, G., Coelho, M., Reis Salles, I., Michel, A., Oliveira, P., Cunha-e-Silva, N., Salmon, D. (2007). Heme requirement and intracellular trafficking in *Trypanosoma cruzi* epimastigotes. Biochem Biophys Res Commun. 355, 16~22.

78. Leach, T. M., Roberts, C. J. (1981). Present status of chemotherapy and chemoprophylaxis of animal trypanosomiasis in the Eastern hemisphere. Pharmacol Ther. 13, 91~147.

79. Legros, D., Ollivier, G., Gastellu-Etchegorry, M., Paquet, C., Burri, C., Jannin, J., Buscher, P. (2002). Treatment of human African trypanosomiasis--present situation and needs for research and development. Lancet Infect Dis. 2, 437-440.

80. Li, T., Bonkovsky, H. L., Guo, J. T. (2011). Structural analysis of heme proteins: implications for design and prediction. BMC Struct Biol. 11, 13.

81. Lindsey, J. S. (2015). De novo synthesis of gem-dialkyl chlorophyll analogues for probing and emulating our green world. Chem Rev. 115, 6534~6620.

82. Magnus, E., Vervoort, T., Van Meirvenne, N. (1978). A card-agglutination test

with stained trypanosomes (C.A.T.T.) for the serological diagnosis of *T. b. gambiense* trypanosomiasis. Ann Soc Belg Med Trop. 58, 169~176.

83. Magona, J. W., Walubengo, J., Odimin, J. T. (2008). Acute haemorrhagic syndrome of bovine trypanosomosis in Uganda. Acta Trop. 107, 186-191.

84. Maines, M. D., Kappas, A. (1977). Metals as regulators of heme metabolism. Science. 198, 1215~1221.

85. Michelotti, E. F., Hajduk, S. L. (1987). Developmental regulation of trypanosome mitochondrial gene expression. J Biol Chem. 262, 927~932.

86. Mogk, S., Meiwes, A., Bosselmann, C. M., Wolburg, H., Duszenko, M. (2014). The lane to the brain: how African trypanosomes invade the CNS. Trends Parasitol. 30, 470~477.

87. Moreira, D., Lopez-Garcia, P., Vickerman, K. (2004). An updated view of kinetoplastid phylogeny using environmental sequences and a closer outgroup: proposal for a new classification of the class Kinetoplastea. Int J Syst Evol Microbiol. 54, 1861~1875.

88. Morgan, G. W., Allen, C. L., Jeffries, T. R., Hollinshead, M., Field, M. C. (2001). Developmental and morphological regulation of clathrin-mediated endocytosis in *Trypanosoma brucei*. J Cell Sci. 114, 2605~2615.

89. Morrison, L. J., Vezza, L., Rowan, T., Hope, J. C. (2016). Animal African trypanosomiasis: Time to increase focus on clinically relevant parasite and host species. Trends Parasitol. 32, 599-607.

90. Mulenga, C., Mhlanga, J. D., Kristensson, K., Robertson, B. (2001).

Trypanosoma brucei brucei crosses the blood-brain barrier while tight junction proteins are preserved in a rat chronic disease model. Neuropathol Appl Neurobiol. 27, 77~85.

91. Murilla, G. A., Mdachi, R. E., Karanja, W. M. (1996). Pharmacokinetics, bioavailability and tissue residues of [14C]isometamidium in non-infected and *Trypanosoma congolense*-infected Boran cattle. Acta Trop. 61, 277~292.

92. Musinguzi, S. P., Suganuma, K., Asada, M., Laohasinnarong, D., Sivakumar, T., Yokoyama, N., Namangala, B., Sugimoto, C., Suzuki, Y., Xuan, X., Inoue, N. (2016). A PCR-based survey of animal African trypanosomosis and selected piroplasm parasites of cattle and goats in Zambia. J Vet Med Sci.

93. Naessens, J. (2006). Bovine trypanotolerance: A natural ability to prevent severe anaemia and haemophagocytic syndrome? Int J Parasitol. 36, 521-528.

94. Neelakanta, G., Sultana, H. (2015). Transmission-Blocking Vaccines: Focus on anti-vector vaccines against tick-borne diseases. Arch Immunol Ther Exp (Warsz). 63, 169-179.

95. Neuberger, A., Meltzer, E., Leshem, E., Dickstein, Y., Stienlauf, S., Schwartz, E. (2014). The changing epidemiology of human African trypanosomiasis among patients from nonendemic countries--1902-2012. PLoS One. 9, e88647.

96. Njiru, Z. K., Mikosza, A. S., Armstrong, T., Enyaru, J. C., Ndung'u, J. M., Thompson, A. R. (2008). Loop-mediated isothermal amplification (LAMP) method for rapid detection of *Trypanosoma brucei rhodesiense*. PLoS Negl Trop Dis. 2, e147.

97. Njiru, Z. K., Ouma, J. O., Bateta, R., Njeru, S. E., Ndungu, K., Gitonga, P. K., Guya, S., Traub, R. (2011). Loop-mediated isothermal amplification test for *Trypanosoma vivax* based on satellite repeat DNA. Vet Parasitol. 180, 358-362.

98. Noireau, F., Lemesre, J. L., Nzoukoudi, M. Y., Louembet, M. T., Gouteux, J. P., Frezil, J. L. (1988). Serodiagnosis of sleeping sickness in the Republic of the Congo: comparison of indirect immunofluorescent antibody test and card agglutination test. Trans R Soc Trop Med Hyg. 82, 237-240.

99. Peacock, L., Cook, S., Ferris, V., Bailey, M., Gibson, W. (2012). The life cycle of *Trypanosoma* (Nannomonas) *congolense* in the tsetse fly. Parasit Vectors. 5, 109.

100. Pentreath, V. W. (1995). Royal society of tropical medicine and hygiene meeting at Manson House, London, 19 May 1994. Trypanosomiasis and the nervous system. Pathology and immunology. Trans R Soc Trop Med Hyg. 89, 9~15.

101. Pentreath, V. W., Baugh, P. J., Lavin, D. R. (1994). Sleeping sickness and the central nervous system. Onderstepoort J Vet Res. 61, 369~377.

102. Pepin, J., Milord, F. (1994). The treatment of human African trypanosomiasis. Adv Parasitol. 33, 1-47.

103. Peretz, D., Williamson, R. A., Matsunaga, Y., Serban, H., Pinilla, C., Bastidas, R. B., Rozenshteyn, R., James, T. L., Houghten, R. A., Cohen, F. E., Prusiner, S. B., Burton, D. R. (1997). A conformational transition at the N terminus of the prion protein features in formation of the scrapie isoform. J Mol Biol. 273,

614~622.

104. Peschle, C., Mavilio, F., Care, A., Migliaccio, G., Migliaccio, A. R., Salvo, G., Samoggia, P., Petti, S., Guerriero, R., Marinucci, M., et al. (1985). Haemoglobin switching in human embryos: asynchrony of zeta----alpha and epsilon----gamma-globin switches in primitive and definite erythropoietic lineage. Nature. 313, 235~238.

105. Ratanasopa, K., Chakane, S., Ilyas, M., Nantasenamat, C., Bulow, L. (2013). Trapping of human hemoglobin by haptoglobin: molecular mechanisms and clinical applications. Antioxid Redox Signal. 18, 2364~2374.

106. Rebeski, D. E., Winger, E. M., Ouma, J. O., Kong Pages, S., Buscher, P., Sanogo, Y., Dwinger, R. H., Crowther, J. R. (2001). Charting methods to monitor the operational performance of ELISA method for the detection of antibodies against trypanosomes. Vet Parasitol. 96, 11-50.

107. Reid, D. G., Jackson, G. J., Duer, M. J., Rodgers, A. L. (2011). Apatite in kidney stones is a molecular composite with glycosaminoglycans and proteins: evidence from nuclear magnetic resonance spectroscopy, and relevance to Randall's plaque, pathogenesis and prophylaxis. J Urol. 185, 725~730.

108. Rodgers, J., McCabe, C., Gettinby, G., Bradley, B., Condon, B., Kennedy, P. G. (2011). Magnetic resonance imaging to assess blood-brain barrier damage in murine trypanosomiasis. Am J Trop Med Hyg. 84, 344~350.

109. Roditi, I., Lehane, M. J. (2008). Interactions between trypanosomes and tsetse flies. Curr Opin Microbiol. 11, 345~351.

110. Rosenblatt, J. E. (2009). Laboratory diagnosis of infections due to blood and tissue parasites. Clin Infect Dis. 49, 1103~1108.

111. Ruepp, S., Furger, A., Kurath, U., Renggli, C. K., Hemphill, A., Brun, R., Roditi, I. (1997). Survival of *Trypanosoma brucei* in the tsetse fly is enhanced by the expression of specific forms of procyclin. J Cell Biol. 137, 1369-1379.

112. Ruttayaporn, N., Zhou, M., Suganuma, K., Yamasaki, S., Kawazu, S., Inoue, N. (2013). Expression and characterization of cathepsin B from tsetse (*Glossina morsitans morsitans*). Jpn J Vet Res. 61, 137~147.

113. Sah, J. F., Ito, H., Kolli, B. K., Peterson, D. A., Sassa, S., Chang, K. P. (2002). Genetic rescue of *Leishmania* deficiency in porphyrin biosynthesis creates mutants suitable for analysis of cellular events in uroporphyria and for photodynamic therapy. J Biol Chem. 277, 14902-14909.

114. Sancovich, H. A., Battle, A. M., Grinstein, M. (1969). Porphyrin biosynthesis. VI. Separation and purification of porphobilinogen deaminase and uroporphyrinogen isomerase from cow liver. Porphobilinogenase an allosteric enzyme. Biochim Biophys Acta. 191, 130-143.

115. Schroeder, W. A., Shelton, J. R., Shelton, J. B., Robberson, B., Babin, D. R. (1967). Amino acid sequence of the alpha-chain of bovine fetal hemoglobin. Arch Biochem Biophys. 120, 1~14.

116. Seed, J. R., Wenck, M. A. (2003). Role of the long slender to short stumpy transition in the life cycle of the african trypanosomes. Kinetoplastid Biol Dis. 2, 3.

117. Shakibaei, M., Milaninezhad, M., Risse, H. J. (1994). Immunoelectron microscopic studies on the specific adhesion of *Trypanosoma congolense* to cultured vascular endothelial cells. J Struct Biol. 112, 125-135.

118. Shemin, D., Russell, C. S., Abramsky, T. (1955). The succinate-glycine cycle. I. The mechanism of pyrrole synthesis. J Biol Chem. 215, 613-626.

119. Shoenfeld, Y., Hsu-Lin, S. C., Gabriels, J. E., Silberstein, L. E., Furie, B. C., Furie, B., Stollar, B. D., Schwartz, R. S. (1982). Production of autoantibodies by human-human hybridomas. J Clin Invest. 70, 205~208.

120. Silverman, J. S., Schwartz, K. J., Hajduk, S. L., Bangs, J. D. (2011). Late endosomal Rab7 regulates lysosomal trafficking of endocytic but not biosynthetic cargo in *Trypanosoma brucei*. Mol Microbiol. 82, 664~678.

121. Simarro, P. P., Diarra, A., Ruiz Postigo, J. A., Franco, J. R., Jannin, J. G. (2011). The human African trypanosomiasis control and surveillance programme of the World Health Organization 2000-2009: the way forward. PLoS Negl Trop Dis. 5, e1007.

122. Simo, G., Herder, S., Cuny, G., Hoheisel, J. (2010). Identification of subspecies specific genes differentially expressed in procyclic forms of *Trypanosoma brucei* subspecies. Infect Genet Evol. 10, 229-237.

123. Souza, W. d. (1999). A short review on the morphology of *Trypanosoma cruzi*: from 1909 to 1999. Mem Inst Oswaldo Cruz. 94 Suppl 1, 17~36.

124. Sowemimo-Coker, S. O. (2002). Red blood cell hemolysis during processing. Transfus Med Rev. 16, 15.

125. Stevens, J. R., Noyes, H. A., Schofield, C. J., Gibson, W. (2001). The molecular evolution of Trypanosomatidae. Adv Parasitol. 48, 1~56.

126. Straka, J. G., Kushner, J. P. (1983). Purification and characterization of bovine hepatic uroporphyrinogen decarboxylase. Biochemistry. 22, 4664~4672.

127. Stuart, K., Brun, R., Croft, S., Fairlamb, A., Gurtler, R. E., McKerrow, J., Reed, S., Tarleton, R. (2008). Kinetoplastids: related protozoan pathogens, different diseases. J Clin Invest. 118, 1301~1310.

128. Suganuma, K., Mochabo, K. M., Hakimi, H., Yamasaki, S., Yamagishi, J., Asada, M., Kawazu, S., Inoue, N. (2013). Adenosine-uridine-rich element is one of the required cis-elements for epimastigote form stage-specific gene expression of the *congolense* epimastigote specific protein. Mol Biochem Parasitol. 191, 36~43.

129. Tetley, L., Vickerman, K. (1985). Differentiation in *Trypanosoma brucei*: host-parasite cell junctions and their persistence during acquisition of the variable antigen coat. J Cell Sci. 74, 1~19.

130. Thekisoe, O. M., Kuboki, N., Nambota, A., Fujisaki, K., Sugimoto, C., Igarashi, I., Yasuda, J., Inoue, N. (2007). Species-specific loop-mediated isothermal amplification (LAMP) for diagnosis of trypanosomosis. Acta Trop. 102, 182-189.

131. Thekisoe, O. M., Omolo, J. D., Swai, E. S., Hayashida, K., Zhang, J., Sugimoto, C., Inoue, N. (2007). Preliminary application and evaluation of loop-mediated isothermal amplification (LAMP) for detection of bovine theileriosis and

trypanosomosis in Tanzania. Onderstepoort J Vet Res. 74, 339-342.

132. Thomsen, J. H., Etzerodt, A., Svendsen, P., Moestrup, S. K. (2013). The haptoglobin-CD163-heme oxygenase-1 pathway for hemoglobin scavenging. Oxid Med Cell Longev. 2013, 523652.

133. Tomas, A. M., Castro, H. (2013). Redox metabolism in mitochondria of trypanosomatids. Antioxid Redox Signal. 19, 696~707.

134. Tripodi, K. E., Menendez Bravo, S. M., Cricco, J. A. (2011). Role of heme and heme-proteins in trypanosomatid essential metabolic pathways. Enzyme Res. 2011, 873230.

135. Trouiller, P., Olliaro, P., Torreele, E., Orbinski, J., Laing, R., Ford, N. (2002). Drug development for neglected diseases: a deficient market and a public-health policy failure. Lancet. 359, 2188~2194.

136. Turinawe, E. B., Rwemisisi, J. T., Musinguzi, L. K., de Groot, M., Muhangi, D., de Vries, D. H., Mafigiri, D. K., Katamba, A., Parker, N., Pool, R. (2016). Traditional birth attendants (TBAs) as potential agents in promoting male involvement in maternity preparedness: insights from a rural community in Uganda. Reprod Health. 13, 24.

137. Ueda, T., Yamada, T., Hokuto, D., Koyama, F., Kasuda, S., Kanehiro, H., Nakajima, Y. (2010). Generation of functional gut-like organ from mouse induced pluripotent stem cells. Biochem Biophys Res Commun. 391, 38~42.

138. Vanhollebeke, B., De Muylder, G., Nielsen, M. J., Pays, A., Tebabi, P., Dieu, M., Raes, M., Moestrup, S. K., Pays, E. (2008). A haptoglobin-hemoglobin

receptor conveys innate immunity to *Trypanosoma brucei* in humans. Science. 320, 677~681.

139. Vreysen, M. J., Seck, M. T., Sall, B., Bouyer, J. (2013). Tsetse flies: their biology and control using area-wide integrated pest management approaches. J Invertebr Pathol. 112 Suppl, S15-25.

140. Welburn, S. C., Molyneux, D. H., Maudlin, I. (2016). Beyond tsetse--Implications for research and control of human African trypanosomiasis epidemics. Trends Parasitol. 32, 230~241.

141. Welchen, E., Gonzalez, D. H. (2016). Cytochrome c, a hub linking energy, redox, stress and signaling pathways in mitochondria and other cell compartments. Physiol Plant. 157, 310~321.

142. Wolburg, H., Mogk, S., Acker, S., Frey, C., Meinert, M., Schonfeld, C., Lazarus, M., Urade, Y., Kubata, B. K., Duszenko, M. (2012). Late stage infection in sleeping sickness. PLoS One. 7, e34304.

143. Wu, Y., Ellis, R. D., Shaffer, D., Fontes, E., Malkin, E. M., Mahanty, S., Fay, M. P., Narum, D., Rausch, K., Miles, A. P. (2008). Phase 1 trial of malaria transmission blocking vaccine candidates Pfs25 and Pvs25 formulated with montanide ISA 51. PloS One. 3, e2636.

144. Yamasaki, S., Suganuma, K., Yamagishi, J., Asada, M., Yokoyama, N., Kawazu, S., Inoue, N. (2016). Characterization of an epimastigote-stage-specific hemoglobin receptor of *Trypanosoma congolense*. Parasit Vectors. 9, 299.